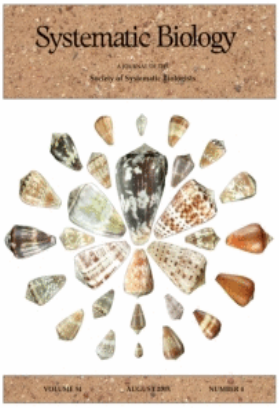

Systematic Biology
Publication details, including instructions for authors and subscription information:
http://www.informaworld.com/smpp/title~content=t713658732

Morphological and Molecular Evidence for a Stepwise Evolutionary Transition from Teeth to Baleen in Mysticete Whales

Thomas A. Deméré [a]; Michael R. McGowen [bc]; Annalisa Berta [b]; John Gatesy [c]
[a] Department of Paleontology, San Diego Natural History Museum, San Diego, California, USA
[b] Department of Biology, San Diego State University, San Diego, California, USA
[c] Department of Biology, University of California, Riverside, California, USA

First Published on: 01 February 2008
To cite this Article: Deméré, Thomas A., McGowen, Michael R., Berta, Annalisa and Gatesy, John (2008) 'Morphological and Molecular Evidence for a Stepwise Evolutionary Transition from Teeth to Baleen in Mysticete Whales', Systematic Biology, 57:1, 15 - 37
To link to this article: DOI: 10.1080/10635150701884632
URL: http://dx.doi.org/10.1080/10635150701884632

Syst. Biol. 57(1):15–37, 2008

ISSN: 1063-5157 print / 1076-836X online
DOI: 10.1080/10635150701884632

Morphological and Molecular Evidence for a Stepwise Evolutionary Transition from Teeth to Baleen in Mysticete Whales

THOMAS A. DEMÉRÉ,[1] MICHAEL R. MCGOWEN,[2,3] ANNALISA BERTA,[2] AND JOHN GATESY[3]

[1]*Department of Paleontology, San Diego Natural History Museum, San Diego, California 92112, USA; E-mail: tdemere@sdnhm.org*
[2]*Department of Biology, San Diego State University, San Diego, California 92182, USA*
[3]*Department of Biology, University of California, Riverside, California 92521, USA*

Abstract.— The origin of baleen in mysticete whales represents a major transition in the phylogenetic history of Cetacea. This key specialization, a keratinous sieve that enables filter-feeding, permitted exploitation of a new ecological niche and heralded the evolution of modern baleen-bearing whales, the largest animals on Earth. To date, all formally described mysticete fossils conform to two types: toothed species from Oligocene-age rocks (∼24 to 34 million years old) and toothless species that presumably utilized baleen to feed (Recent to ∼30 million years old). Here, we show that several Oligocene toothed mysticetes have nutrient foramina and associated sulci on the lateral portions of their palates, homologous structures in extant mysticetes house vessels that nourish baleen. The simultaneous occurrence of teeth and nutrient foramina implies that both teeth and baleen were present in these early mysticetes. Phylogenetic analyses of a supermatrix that includes extinct taxa and new data for 11 nuclear genes consistently resolve relationships at the base of Mysticeti. The combined data set of 27,340 characters supports a stepwise transition from a toothed ancestor, to a mosaic intermediate with both teeth and baleen, to modern baleen whales that lack an adult dentition but retain developmental and genetic evidence of their ancestral toothed heritage. Comparative sequence data for *ENAM* (enamelin) and *AMBN* (ameloblastin) indicate that enamel-specific loci are present in Mysticeti but have degraded to pseudogenes in this group. The dramatic transformation in mysticete feeding anatomy documents an apparently rare, stepwise mode of evolution in which a composite phenotype bridged the gap between primitive and derived morphologies; a combination of fossil and molecular evidence provides a multifaceted record of this macroevolutionary pattern. [ameloblastin (*AMBN*); baleen; enamelin (*ENAM*); evolution; filter-feeding; Mysticeti; whale.]

Recent discoveries of early whale fossils have provided remarkable examples of macroevolutionary change at the base of the cetacean family tree (e.g., Gingerich et al., 2001; Thewissen and Williams, 2002). For Mysticeti (baleen whales), it is predicted that archaic forms should preserve intermediate stages in the transition from primitive, tooth-aided predation to derived, filter-feeding using baleen. The origin of filter-feeding represents a major morphological and ecological shift in mammalian evolution; by efficiently batch-feeding, mysticetes gained access to huge energy resources. Ultimately, the novel filter-feeding strategy permitted the evolution of gigantic body size, a hallmark of modern baleen whales (Werth, 2000). Exactly how the fundamental reorganization of feeding anatomy occurred is unclear, in part because crucial transitional fossils have not been adequately described, formally characterized, and incorporated into comprehensive phylogenetic analyses.

Baleen is a defining feature of modern mysticetes; extant species use this unique filtering structure to consume as much as 600,000 kg of prey in a year (Gaskin, 1982). Although epidermal in origin, baleen is not homologous to teeth. Rather, it is a tough keratinous material that is secreted from gingival epithelia of the palate and typically forms right and left racks of transversely oriented plates that extend into the oral cavity (Utrecht, 1965). Movements of the tongue abrade the lingual surfaces of the continuously growing baleen plates. This abrasion exposes the individual keratinous tubules within the medulla layer of the cornified plates, resulting in a matted network of fringe on the medial margin of the baleen racks. When the jaws are not completely closed, the frayed baleen functions as a sieve that entraps prey items but allows water to pass out of the mouth (Pivorunas, 1979). All extant mysticetes are edentulous (toothless) as adults and utilize their baleen racks, in combination with other unique anatomical and behavioral specializations, to capture aggregations of small fish, invertebrates, or both (Werth, 2000).

The earliest known edentulous mysticetes (*Eomysticetus*, *Micromysticetus*, and *Mauicetus*) have been recovered from Late Oligocene-age rocks (∼24 to 30 million years old [Ma]) of South Carolina, USA (Sanders and Barnes, 2002a, 2002b), and New Zealand (Fordyce, 1982, 2006). However, the fossil record also has yielded mysticetes with teeth from Late to Early Oligocene-age rocks (∼24 to 34 Ma). These include aetiocetids from the North Pacific (Barnes et al., 1995) and members of Mammalodontidae, Janjucetidae, and Llanocetidae from the Southern Ocean (Pritchard, 1939; Mitchell, 1989; Fordyce and Muizon, 2001; Fordyce, 2003a; Fitzgerald, 2006). Most previous studies suggested that these toothed mysticetes lacked baleen and either filtered prey items with their multicusped teeth in the manner of the living crabeater seal, *Lobodon carcinophagus* (Fordyce, 1984, 1989; Mitchell, 1989; Fordyce and Barnes, 1994; Barnes et al., 1995; Ichishima, 2005), or fed similarly to odontocetes (toothed whales) by suction or tooth-aided grasping of isolated prey (Werth, 2000; Arnold et al., 2005b; Fitzgerald, 2006). Fordyce (1984) speculated that baleen might have been present in some toothed mysticetes but noted the absence of anatomical evidence in support of this hypothesis.

Although baleen rarely fossilizes, bony vascular structures on the palate of edentulous mysticetes generally are interpreted as osteological correlates for the presence of baleen (Kellogg, 1965; Fordyce and Muizon, 2001;

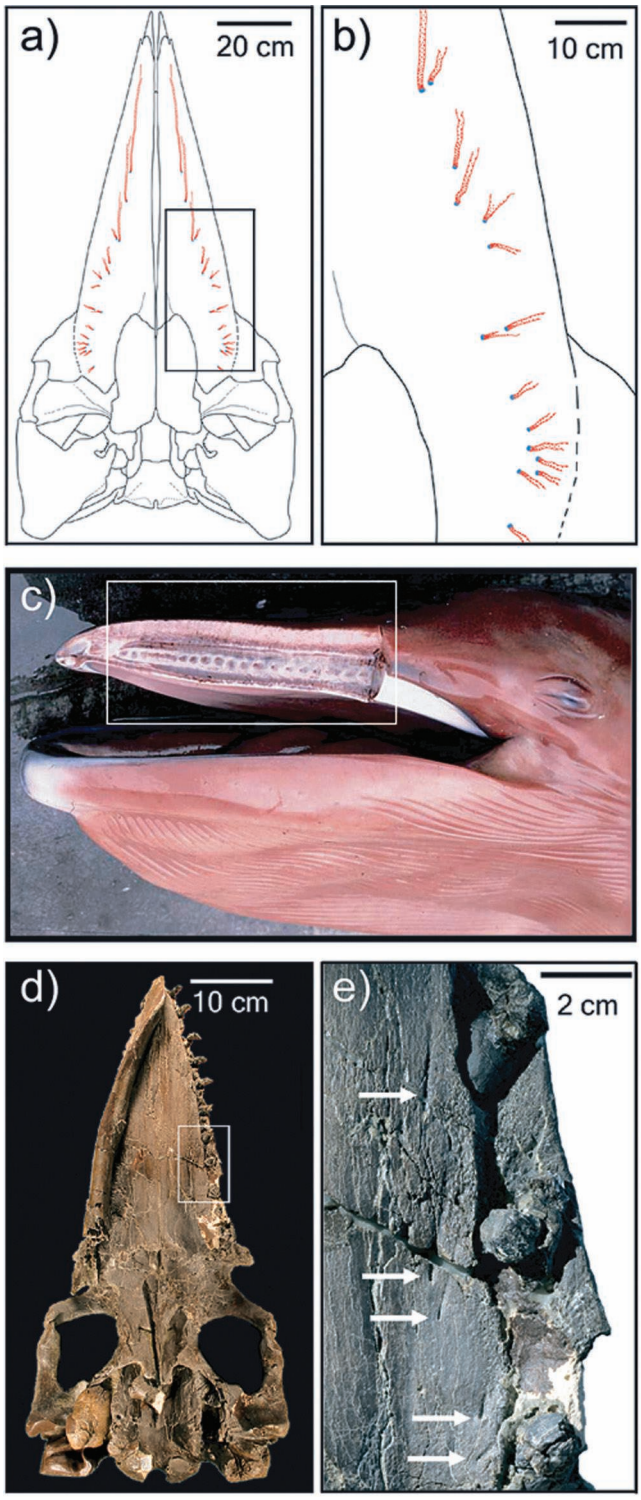

FIGURE 1. Mysticete palates and dentitions. (a, b) sketch of palate from an extant edentulous mysticete (*Balaenoptera acutorostrata*—minke whale); (c) lateral view of a mysticete fetus (*Balaenoptera physalus*—fin whale) with dissection showing tooth buds in upper jaw; and (d, e) palate of the holotype of *Aetiocetus weltoni* (UCMP 122900; ~24 to 28 million years old). b is an enlargement of the inset in a (blue = lateral nutrient foramen; red = sulcus). e is an enlargement of the inset in d; white arrows point to nutrient foramina and associated sulci. Photo of *Balaenoptera physalus* is by Alex Aguilar (GRUMM/FDS).

Fitzgerald, 2006). In extant taxa, foramina on the medial portion of the palate (palatine and maxillary) conduct the descending palatine artery and nerve. In contrast, the lateral portion of the palate (maxillary only) is marked by a series of nutrient foramina and associated vascular grooves/sulci that provide passage for branches of the superior alveolar artery and nerve (Fig. 1a, b). The blood vessels of the superior alveolar artery nourish the epithelia from which the continually growing baleen develops (Walmsley, 1938). Thus, the medially placed foramina represent the generalized mammalian palatine foramina, whereas the lateral nutrient foramina can be considered a neomorphic feature unique to baleen-bearing mysticetes.

Lateral nutrient foramina are not present on the maxilla of early fetal specimens of extant balaenopterid mysticetes. Instead, there is a single open alveolar groove running along the lateral edge of the flat palate where a rudimentary dentition develops (Ridewood, 1923). The tooth germs pass through the bud, cap, and bell stages of development (Fig. 1c) but fail to reach the crown (maturation) stage before degradation by odontoclasts and macrophages (Karlsen, 1962; Ishikawa and Amasaki, 1995; Ishikawa et al., 1999). In the minke whale (*Balaenoptera acutorostrata*), odontoblasts begin to secrete dentin during the bell stage, but there is no subsequent formation of enamel (Ishikawa et al., 1999). Dermal papillae of the primordial baleen plates begin to develop coincident with tooth bud degeneration, while at the same time the open alveolar groove on the palate progressively ossifies until only the distinct lateral nutrient foramina remain. Both upper and lower teeth develop in the fetus, never break the gum line, and ultimately are resorbed before birth (Ridewood, 1923; Dissel-Scherft and Vervoort 1954; Slijper, 1962; Karlsen, 1962; Ishikawa et al., 1999). Thus, modern mysticetes pass through a stage with teeth only (Fig. 1c), to teeth and baleen plate germs, to baleen only; the first two stages occur in utero, whereas the last stage is observed in juveniles and adults (Ishikawa and Amasaki, 1995; Ishikawa et al., 1999). This developmental series could represent an ancient evolutionary character transformation that is recapitulated in the ontogeny of extant mysticetes. However, most recent phylogenetic analyses of Mysticeti instead imply a direct saltatory transition from an ancestral form with tooth-lined jaws to the modern condition where the jaws are toothless with right and left racks of baleen suspended from the palate (Kimura and Ozawa, 2002; Sanders and Barnes, 2002a; Geisler and Sanders, 2003; Bisconti, 2005, 2007; Bouetel and Muizon, 2006; Steeman, 2007).

The shift to a filter-feeding strategy in Mysticeti included extensive changes in anatomy and behavior but also must have involved evolutionary change at the molecular level. In particular, dental genes should register a release from selective constraints with the loss of functional teeth. The secretory calcium-binding phosphoprotein (SCPP) gene family includes several linked genes that are essential for proper development of the dentition (Kawasaki and Weiss, 2003; Kawasaki et al., 2004; Huq et al., 2005). *DMP1* (dentin matrix acidic phosphoprotein) is expressed in tooth dentin but also

more broadly in skeletal tissues; normal development of dentin, cartilage, and bone is disrupted by null mutations of the *DMP1* gene (Feng et al., 2003; Massa et al., 2005; Ye et al., 2005). *AMBN* and *ENAM* encode ameloblastin and enamelin respectively, extracellular matrix proteins found in developing enamel; mutants of these SCPP genes are associated with dental defects, such as amelogenesis imperfecta where the malformed enamel can be thin, rough, and hypocalcified (Mårdh et al., 2002; Hu and Yamakoshi, 2003; Fukumoto, et al., 2004; Kim et al., 2005; Masuya et al., 2005). Although dentin is produced in the transient teeth of fetal baleen whales, enamel apparently is not (Dissel-Scherft and Vervoort 1954; Karlsen, 1962; Ishikawa and Amasaki, 1995; Ishikawa et al., 1999). Given that edentulous mysticetes recently descended from ancestors with fully mineralized dentitions, we predicted that enamel-specific SCPP genes would be present, but not functional, in modern baleen whales.

The objectives of this study are the following. First, we document new observations of palatal anatomy in Oligocene aetiocetid mysticetes that represent a critical link in the transition from tooth-assisted predation to filter-feeding with baleen. Second, we PCR amplify and characterize sequences of 11 nuclear loci, including three SCPP dental genes, from the genomes of edentulous baleen whales. Third, we integrate the newly generated morphological and molecular evidence into a character/taxon supermatrix for Mysticeti. Finally, we execute phylogenetic analyses of this combined database to reconstruct the macroevolutionary transformation from teeth to baleen in mysticete whales.

Materials and Methods

New Observations of Toothed Mysticete Palates

Among aetiocetid mysticetes, the holotype of *Aetiocetus weltoni* (UCMP 122900; ~24 to 28 Ma) has the most completely preserved palate and dentition. When this species was first described (Barnes et al., 1995), the palatal anatomy of the holotype was obscured by the closely articulated lower jaws and intervening sedimentary matrix. With the permission of the University of California Museum of Paleontology (UCMP), we removed the left dentary from the skull along with the surrounding mudstone matrix to reveal the well-preserved palatal surface (Figs. 1d, e and 2). We then compared the anatomy of *A. weltoni* to that of other toothed mysticetes (*Aetiocetus cotylalveus, Aetiocetus polydentatus, Chonecetus goedertorum, Mammalodon colliveri*, and *Janjucetus hunderi*), edentulous mysticetes, odontocetes, and an "archaeocete" (see Appendix 1).

SCPP Loci (Dental Gene Matrix)

Past research suggests that extant mysticetes do not produce enamel (Dissel-Scherft and Vervoort 1954; Karlsen, 1962; Ishikawa and Amasaki, 1995; Ishikawa et al., 1999). Therefore, it might be expected that baleen whales would lack enamel-specific genes or that these loci would be degraded pseudogenes. We attempted to PCR amplify and sequence segments of four SCPP exons (*AMBN* exons 6 and 13, *ENAM* exon 9, and *DMP1* exon 6) from 13 edentulous mysticete species and 12 outgroup taxa. Published data from another six mammalian species were included in phylogenetic analyses of the three dental genes (see Appendix 1 for complete list of taxa and sources of DNA samples).

PCR primers for SCPP genes are shown in Table 1. PCR reactions were done in 50-μL volumes and contained 67 mM Tris, 3 mM $MgCl_2$, 16.6 mM $(NH_4)_2SO_4$, 200 μM dNTPs, 2 μM of each primer, and 0.5 to 1.0 U of *Taq* polymerase (Invitrogen). Amplifications included an initial denaturation phase at 94°C (2 min); followed by 45 to 50 cycles at 94°C (1 min), 53°C to 58°C (1 min), 72°C (1 min); and a final elongation phase at 72°C (2 min). PCR products were cleaned and concentrated using Montage PCR Centrifugal Filter Devices (Millipore) and were sequenced in both directions. Contigs were assembled in MacVector 7.2.3 (Accelrys), and heterozygous sites were coded as IUPAC ambiguities. Some PCR amplifications did not produce a concentrated product that sequenced cleanly. In these cases, the PCR product was cloned using pCR 4-TOPO vector (Invitrogen), minimally three clones were sequenced, and a consensus was derived for subsequent analyses. We used MacVector 7.2.3 for conceptual translation of DNA sequences and for identification of premature stop codons in mysticete dental genes. All new data were submitted to GenBank (accession nos. EU444965-EU445012, EU445026-EU445074).

Orthologous sequences were aligned using Clustal W (Thompson et al., 1994) as implemented in MacVector 7.2.3. Gap-opening penalty was set at 10, gap extension penalty was 1, and default settings were used for other alignment parameters. Minor adjustments were made to the algorithmic alignments by eye using SeqApp 1.9a (Gilbert, 1992). Gaps in final alignments were assigned character states using the "simple gap coding" procedure (Simmons and Ochoterena, 2000) that is implemented in SeqState v.1.25 (Müller, 2005). Aligned sequences and gap characters from *AMBN*, *DMP1*, and *ENAM* were merged into a single data set of 1,708 nucleotide positions for 31 operational taxonomic units (OTUs). This "dental gene matrix" was submitted to Morphobank (http://morphobank.geongrid.org). Data for the three SCPP dental genes also were incorporated into the combined mysticete supermatrix (see below).

Combined Morphological and Molecular Data (Mysticete Supermatrix)

Comparative morphological and molecular data for Mysticeti and outgroups were integrated into a combined systematic supermatrix (e.g., Lee, 2005). For extant taxa, we surveyed three dental genes from the SCPP family (see above) and eight additional nuclear loci (*ATP7A, BDNF, CSN2, PKDREJ, PRM1, KITLG, RAG1, STAT5A*); 102 morphological characters were coded for both fossil and living species. We merged these data with published systematic evidence including coloration patterns (Arnold et al., 2005a), insertions of transposons (Nikaido

TABLE 1. PCR primers utilized in this study (5′ to 3′). For each gene fragment, alternative combinations of forward and reverse primers were used to amplify orthologous DNA fragments from different mammalian species; citations for published primers are noted. PCR amplifications with the second *RAG1* forward primer were sequenced with the third *RAG1* forward primer listed below.

Gene	Forward primers	Reverse primers
DMP1	CAAGACCCCAGCAGCGAGTC	CATCTTGGCAATCATTGTCATC
		TCTCCGATGGGTTTGTTGTG
AMBN	TATGAATATTCTTTGCCTGTGC	CTTTGGTGGCTTTTCTGATG
(exon 6)	CTCAACAGCCAGGACAGAA	
AMBN	AGGATTTGGAGGCATGAGG	TCAGGGCTCTTGGAAATGC
(exon 13)	GCTCAGCCTTGGAGGGATG	TCAGGGCTCTTGGAAACGC
		GTGAATCATGCTTAATCTGG
ENAM	TCCTGCTGGAAGAAATACTTGG	TGGCRTAATAGCCCCTGCTC
		GCATTRTTRGCATARTAGCCC
ATP7A	Murphy et al., 2001	Murphy et al., 2001
BDNF	Murphy et al., 2001	Murphy et al., 2001
CSN2	Gatesy et al., 1996	Gatesy et al., 1996
	Gatesy and Arctander, 2000	Gatesy and Arctander, 2000
KITLG	Matthee et al., 2001	Matthee et al., 2001
PKDREJ	CCGTGAGGATAAATAGGAACGACG	CAGATACACCCCCCAAGGTAAAG
	CAAAAGTGTGAGTATAGGACCG	GATATAGTGAGGATCGAAAGGAATG
PRM1	Queralt et al., 1995	Queralt et al., 1995
		GTGGCAAGAGGGTCTTGAAG
RAG1	ACTTCCTGGCCAGACCTCATTGC	ACACGGATGGCCAAGCAAACAGCTG
	TGACTCGATCCATCCCACTGAGTTCTG	AGCTCGTCAGCTTGTCTGTGCTC
	TGACTCGATCCATCCCACT	
STAT5A	Matthee et al., 2001	Matthee et al., 2001

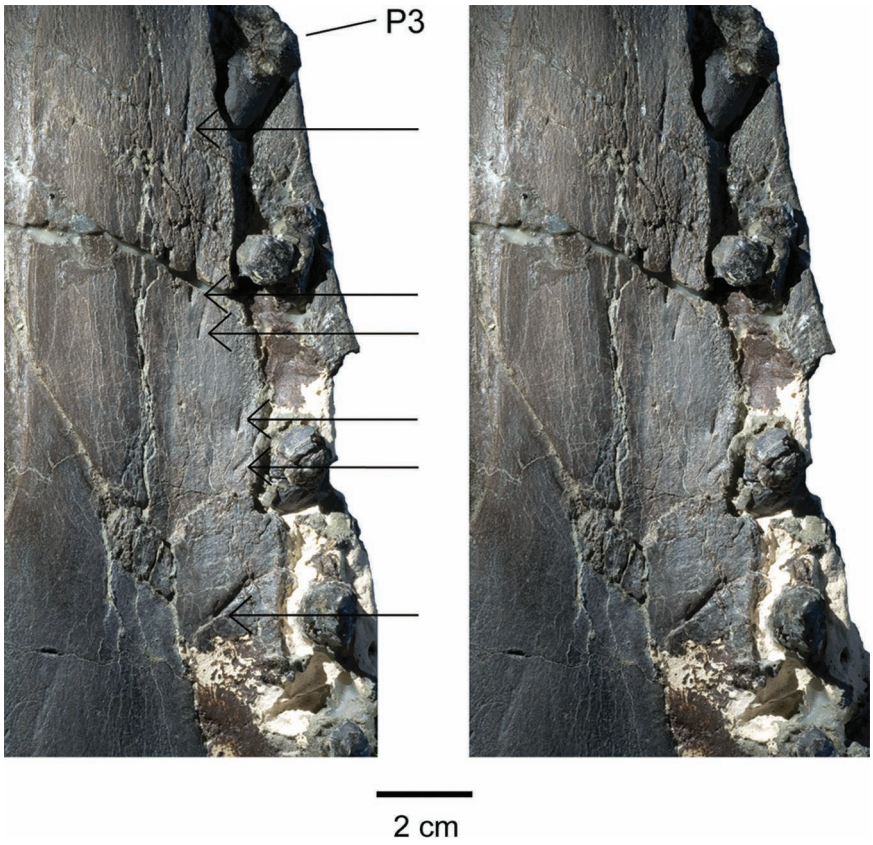

FIGURE 2. Stereopair photograph of left side of palate of *Aetiocetus weltoni* (UCMP 122900). Arrows point to the six posterior-most nutrient foramina (P3 = third upper premolar).

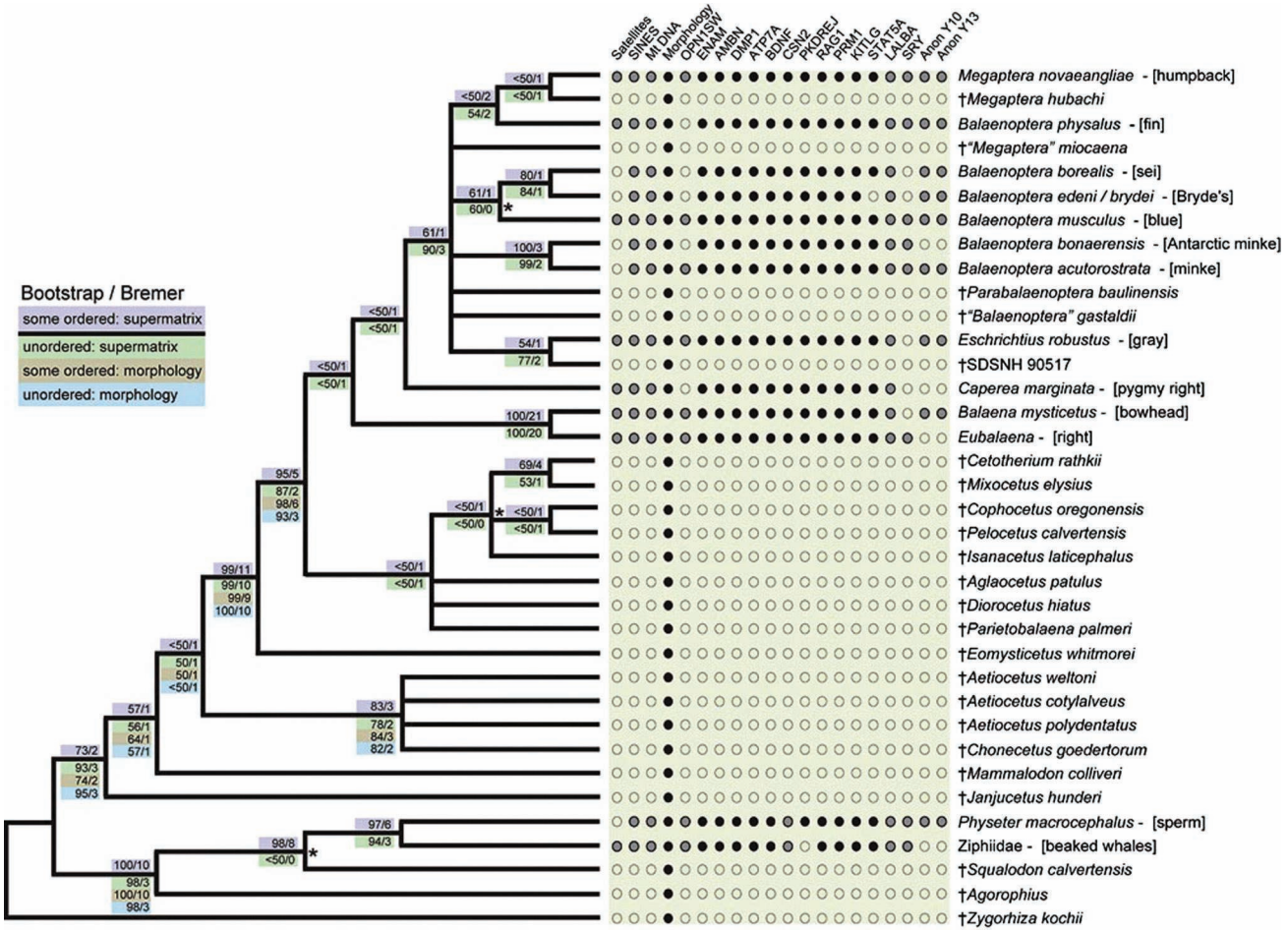

FIGURE 3. Strict consensus tree derived from parsimony analysis of the mysticete supermatrix (some characters ordered). With all characters unordered, the three nodes with asterisks collapsed. Black and gray circles indicate which data sets (top) were sampled for each taxon. Black circles specify character data collected for this paper, and gray circles designate previously published data. Because the majority of species are extinct, most molecular data are missing, and morphology is the only partition coded for all taxa. Numbers at internodes show parsimony bootstrap percentage and Bremer support for different analyses: purple = supermatrix with some characters ordered; green = supermatrix with all characters unordered; orange = morphology with some characters ordered; and blue = morphology with all characters unordered. Support scores for the morphological partition are shown only at critical basal nodes. Common names for extant taxa are in brackets to the right, and extinct taxa are marked by "†."

et al., 2006), mitochondrial (mt) genomes (Árnason et al., 2004; Sasaki et al., 2005, 2006), and a diversity of nuclear DNA sequences (Árnason et al., 1992; Nishida et al., 2003; Levenson and Dizon, 2003; Rychel et al., 2004; Hatch et al., 2006). The supermatrix for Mysticeti included 27,340 systematic characters that summarize the physical and genomic attributes of 31 mysticete taxa (11 extant and 20 extinct) and five representatives of outgroup taxa (Figs. 3, 4; Appendix 1 shows sources of DNA samples and museum specimens examined; see Appendix 2 for morphological character list).

PCR, sequencing, alignment, and gap-coding protocols for all nuclear loci were as described above (SCPP Loci [Dental Gene Matrix]), except that PCR annealing temperature for the *RAG1* gene was higher (59°C to 63°C). PCR primers for *ATP7A* (exon), *BDNF* (exon), *CSN2* (exon), *PKDREJ* (exon), *PRM1* (exon and intron), *KITLG* (exon and intron), *RAG1* (exon), and *STAT5A* (exon and intron) are indicated in Table 1. For the mysticete supermatrix, newly generated DNA sequences (6083 nucleotide positions) and associated gap characters were combined with our morphological data and published systematic evidence; extinct taxa were coded as missing (?) for all molecular characters (Fig. 3). New DNA sequences were submitted to GenBank (accession nos. EU444877-EU445074), and the mysticete supermatrix was stored at Morphobank (http://morphobank.geongrid.org).

Phylogenetic Analyses and Character Mapping

Parsimony analyses of the supermatrix (36 OTUs; 27,340 characters; 3574 parsimony-informative characters) and the dental gene matrix (31 OTUs; 1750 characters; 698 parsimony-informative characters) were executed in PAUP* 4.0b10 (Swofford, 2002). For

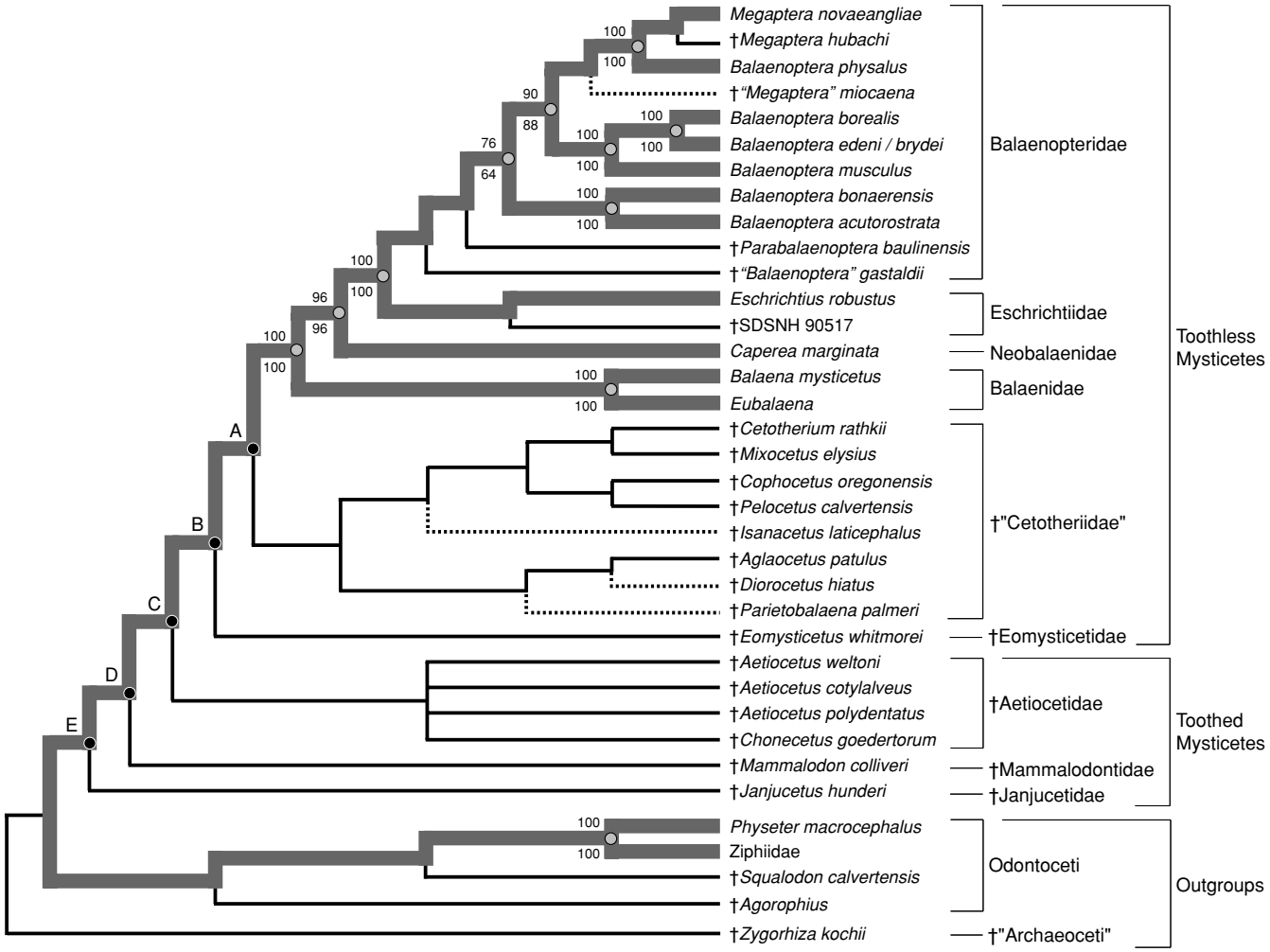

FIGURE 4. One of six optimal cladograms derived from parsimony analysis of the mysticete supermatrix (some characters ordered). Dashed branches connect to four species that were unstable in this analysis and accounted for incomplete resolution of the strict consensus (Fig. 3). Relationships among the remaining 32 taxa were identical in all minimum length topologies. Thick gray branches highlight lineages that connect extant taxa, and light gray circles mark nodes that define relationships among these taxa. Parsimony bootstrap percentages at internodes are for supermatrix analyses of the extant taxa only (above = some characters ordered; below = all characters unordered). Higher-level taxa are delimited by brackets to the right, and wholly extinct taxa are marked by "†." Capital letters at nodes with black circles (A to E) indicate subclades of Mysticeti discussed in the text. The following characters (Appendix 2) were unique and unreversed synapomorphies for these groups in all optimal trees supported by the supermatrix (clade A: 23; clade B: 5, 22, 36, 61, 79, 83; clade C: 38; clade D: 4; clade E: 41, 42, 53). The antiquity of the earliest edentulous mysticetes (Sanders and Barnes, 2002a, 2002b; Fordyce, 2006) suggests that clade B is ∼28 Ma or older.

the mysticete supermatrix, the "archaeocete" *Zygorhiza kochii* was used as the outgroup (Geisler and Sanders, 2003), and for the dental gene matrix, members of Euarchontoglires (*Homo sapiens* + *Mus musculus* + *Rattus norvegicus*) rooted the remaining 27 taxa (Murphy et al., 2001). In most analyses, character state changes were given equal weight. Characters generally were unordered, but supplementary analyses of the supermatrix checked the influence of ordering a subset of the morphological characters (see Appendix 2). Parsimony searches were heuristic with ≥500 random stepwise-addition replicates and tree bisection reconnection (TBR) branch swapping. Internal branches were collapsed if minimum length was zero ("amb-" option), and strict consensus trees were used to summarize relationships supported by all minimum length topologies. Additional tree searches were executed for individual subpartitions of the supermatrix (e.g., *CSN2* gene, mtDNA, morphology, extant taxa only).

Support in the parsimony framework was evaluated by Bremer support scores (Bremer, 1994) and by nonparametric bootstrapping (Felsenstein, 1985). For Bremer support calculations, parsimony analyses were as described above, but with 50 to 100 random stepwise additions, using PAUP* and TreeRot.v2c (Sorenson, 1999). In each bootstrap analysis, only parsimony-informative characters were considered. One thousand pseudoreplicates were executed, and for each bootstrap iteration, the search was heuristic with 10 random stepwise additions and TBR branch swapping.

Markov chain Monte Carlo (MCMC) Bayesian analysis of the dental gene matrix was conducted using MrBayes 3.1.1 (Ronquist and Huelsenbeck, 2003). The data set was divided into two partitions: aligned nucleotides and gap characters. A single model was utilized for sequences from *DMP1*, *AMBN*, and *ENAM*; the GTR+I+G model was selected according to the Akaike information criterion in MrModelTest v2 (Nylander, 2004). The "binary" model was implemented for associated gap characters. Partitioned Bayesian analysis used default priors and was run for 5,000,000 generations. Trees were sampled every 100 generations, the first 10,000 trees were discarded as burn-in following visual inspection of output, and a 50% majority rule consensus of the remaining trees was taken to summarize posterior probabilities for each clade.

To reconstruct the sequence and timing of evolutionary changes in Mysticeti, we optimized character state changes onto phylogenetic hypotheses by parsimony using PAUP* (Swofford, 2002). In particular, we mapped (1) anatomical changes that may be related to filter-feeding in Mysticeti (Fordyce, 1982, 2003b; Barnes et al., 1995; Bouetel, 2005; Fitzgerald, 2006), and (2) insertions and deletions (indels) in dental genes. For morphological characters, we utilized trees supported by analyses of the mysticete supermatrix. For optimization of molecular changes in dental genes, we employed two trees. The first topology was the majority rule consensus from the Bayesian analysis of the dental gene matrix. This topology also was one of the minimum length parsimony trees for the dental gene matrix, but because relationships within Mysticeti were unconventional and sharply conflicted with our supermatrix results, we also utilized a second, composite tree. In this topology, relationships among outgroups to Mysticeti were those favored by Bayesian analysis of the dental gene matrix, and relationships among extant mysticetes were those supported by parsimony analysis of the more comprehensive supermatrix.

RESULTS

New Observations of Toothed Mysticete Palates

Lateral nutrient foramina and associated sulci have not been documented in previously published descriptions of fossil-toothed mysticetes (Pritchard, 1939; Fordyce, 1982, 1984, 1989; 2003a; Mitchell, 1989; Barnes et al., 1995; Ichishima, 2005; Fitzgerald, 2006), but we discovered these features in three Oligocene aetiocetids (also see Deméré, 2005; Deméré et al., 2006). In the holotype skull of *Aetiocetus weltoni* (UCMP 122900; Figs. 1d, e and 2), the anterior teeth (I1–P1) are roughly caniniform with sharply pointed, simple crowns; the posterior teeth (P2–M3) are transversely compressed, more broadly triangular, and topographically complex with fine anterior and posterior denticles. A series of eight lateral nutrient foramina occurs slightly medial to the left tooth row between C and M2 (the right mandible is still articulated with the skull and obscures the right side of the palate). The following description of the nutrient foramina begins with the posteriormost foramen (no. 1) and proceeds to the anteriormost foramen (no. 8). Foramen no. 1 is small (∼1 mm diameter), located ∼10 mm from the medial alveolar margin of M2, and opens into a fine, anterolaterally oriented sulcus ∼11 mm in length that forms an angle of ∼40° with the sagittal plane. Anterior to foramen no. 1, two foramina of the same small diameter (∼1 mm) are positioned ∼3 mm from M1. The posterior foramen of this pair (no. 2) and its sulcus (∼2.5 mm long) form an angle of ∼60° with the sagittal plane, while the other foramen (no. 3) occurs 6 mm anterior to no. 2 with an anteriorly directed sulcus (∼6.5 mm long) that is angled ∼25° to the sagittal plane. Another pair of small (∼1 mm diameter) foramina (no. 4 and no. 5) occurs ∼9 mm from the medial edge of P4; sulci associated with these delicate foramina form an angle of ∼20° with the sagittal plane and measure ∼8.5 and 5.5 mm, respectively. A larger foramen (no. 6) ∼1.5 mm in diameter is positioned ∼7 mm from the posteromedial corner of the exposed P3 root, and the associated sulcus (∼15.5 mm long) angles ∼10° to the sagittal plane. Another large foramen (∼2 mm diameter) occurs within 4 mm of the medial alveolar border of P2. The associated sulcus of this foramen (no. 7) is short (∼7 mm long), less distinct relative to those associated with the more posterior foramina, and roughly parallel to the sagittal plane. The anteriormost foramen (no. 8) occurs ∼3 mm medial to the diastema between the C and P1. This foramen is of small caliber (∼1 mm diameter), and its associated sulcus is poorly formed and oriented roughly parallel to the sagittal plane. Thus, the general maxillary vascularization pattern consists of a roughly radial orientation of sulci through an arch of ∼50° (i.e., forming angles with the sagittal plane of 10° to 60°) in the posterior half of the palate (Fig. 2) and a more parasagittal orientation of sulci in the anterior portion of the palate. Relative to edentulous mysticetes, this pattern is most similar to that of balaenopterids (Fig. 1a, b) and fossil "cetotheres" (see below).

We also observed lateral nutrient foramina and sulci of similar size and orientation in two other Oligocene aetiocetids, *Aetiocetus cotylalveus* and *Chonecetus goedertorum*, but preservation of the palate in these specimens was much poorer than in UCMP 122900. Only one obvious nutrient foramen was found on the palate of *Aetiocetus cotylalveus* (United States National Museum; USNM 25210) and occurs on the right maxilla adjacent to the P4–M1 diastema, ∼3 mm from the medial margin of the M1 alveolus. The associated sulcus forms an angle of ∼5° with the sagittal plane and measures ∼13 mm in length. The holotype skull of *Chonecetus goedertorum* (Natural History Museum of Los Angeles County; LACM 131146) preserves three distinct lateral nutrient foramina. One on the right maxilla between P2 and P3 is filled with matrix, lies ∼2 to 3 mm from the medial margins of the alveoli, and opens anteriorly into a delicate sulcus that is oriented ∼4° to the sagittal plane. A second foramen occurs on the left maxilla adjacent to the M2 alveolus; the matrix filled sulcus is anterolaterally oriented ∼40° to the sagittal plane and measures ∼5 mm in length. A

third foramen occurs on the left maxilla adjacent to the P4 alveolus, ~1 mm from its medial margin. The associated sulcus is approximately parallel to the sagittal plane and is ~7 mm long. We did not find nutrient foramina and associated sulci in *Aetiocetus polydentatus* (Ashoro Museum of Paleontology; AMP 12), the fourth aetiocetid that we examined. The preparation of this fossil is not complete, however, and the relatively poor preservation of the palate might not allow detection of delicate foramina like those seen in *A. weltoni* (Figs. 1e and 2). In our supermatrix analysis, we coded *A. polydentatus* as equivocal (?) for character no. 38, presence/absence of nutrient foramina on the palate (Appendix 2).

Lateral nutrient foramina evidently are widespread in Aetiocetidae. In a recent meeting abstract, Sawamura et al. (2006) cited the presence of these features in close association with the dentition of an undescribed species of *Morawanocetus* (Aetiocetidae) from the Late Oligocene of Hokkaido, Japan (AMP14). A thorough account of the palatal vascularization has not been published; however, it is noteworthy that a third aetiocetid genus apparently expresses lateral nutrient foramina. Such foramina have not been reported from members of other toothed mysticete families. Fordyce (2003a) observed "abundant fine grooves around the alveoli" of the upper teeth in the holotype skull of *Llanocetus denticrenatus* (Llanocetidae) but did not specify the presence of nutrient foramina in this Early Oligocene mysticete (~34 Ma). A detailed description currently is lacking, and it is not yet clear whether the fine palatal grooves of *Llanocetus* are homologous to the sulci associated with baleen in extant species (Fig. 1a, b). In another meeting abstract, Barnes and Sanders (1996) announced the discovery of archaic toothed mysticetes from the eastern United States (The Charleston Museum; ChMPV5720 and ChM PV4745). These undescribed fossils, as well as members of Mammalodontidae and Janjucetidae, are reported to lack lateral nutrient foramina and associated sulci (Geisler and Sanders, 2003; Fitzgerald, 2006).

Observations of Palate Vascularization in Edentulous Mysticetes and in Odontocetes

Lateral nutrient foramina are present in all recent mysticetes. In most extant species of Balaenopteridae (rorquals), the distinct sulci associated with the lateral nutrient foramina (~10 to 17 per side) have a general radial orientation through an arch of ~85° (i.e., forming angles with the sagittal plane from 15° to 100°) in the posterior half of the palate and a more parasagittal orientation in the anterior portion of the palate (Fig. 1a, b). Although the anterior maxillary vascularization in extant members of Eschrichtiidae (gray whales), Balaenidae (right and bowhead whales), and Neobalaenidae (pygmy right whales) also consists of parasagittally oriented, elongate, and somewhat en echelon sulci, the posterior maxillary vascularization patterns in these taxa are distinct. The eschrichtiid condition roughly involves two parallel rows of irregularly shaped and variably sized foramina (>25 per side), with very short to nonexistent sulci. The balaenid pattern consists of widely spaced single, circular foramina that lack well-formed sulci. Slightly medial to these foramina lies a longitudinal maxillary groove that is open posteriorly to the back edge of the infraorbital plate. Short, curved sulci extend laterally from this open groove across the surface of the maxillary. The axis of the groove aligns with the parasagittally oriented sulci at the front of the palate. In the only extant neobalaenid, *Caperea marginata*, the posterior maxillary vascularization pattern includes numerous (>25 per side) transversely oriented sulci that originate medially from a nearly continuous, longitudinal maxillary groove. In contrast to the condition in balaenids, the neobalaenid maxillary groove does not extend to the posterior edge of the infraorbital plate of the maxilla.

Although not always well preserved and adequately prepared, lateral nutrient foramina and sulci have been reported in a number of fossil edentulous mysticetes. The majority of these reports are of Miocene "cetotheres" and generally describe a pattern of posterior, radially arranged sulci with anterior, parasagittally oriented, elongate sulci (Kellogg, 1934, 1965, 1968a, 1968b, 1968c; Kimura and Ozawa, 2002; Bouetel and Muizon, 2006; Deméré pers. obs.). This condition is most like that of extant balaenopterids, except that in many of the "cetotheres," the posterior sulci are distinctly longer.

In the "archaeocete" outgroup, *Zygorhiza*, and in all extant and extinct odontocetes that we have examined, lateral nutrient foramina and sulci are absent. The patterns of palatal vascularization in ziphiids (beaked whales) and physeterids (sperm whales), however, deserve a more expanded discussion. In extant members of both groups, maxillary teeth are typically rudimentary (Boschma, 1938, 1950, 1951) and when present do not insert into distinct bony alveoli (*Tasmacetus sheperdi* is an exception). Instead, the teeth are embedded in soft palatal tissues and generally do not erupt (Flower, 1869, 1878; Rice, 1989). To our knowledge, detailed comparative studies of the palate vascular patterns in beaked and sperm whales are lacking, but it is possible to offer some general observations here.

In ziphiids with a rudimentary maxillary dentition (e.g., *Mesoplodon* spp.), a remnant alveolar groove is present. Ziphiid morphologists call this the "basirostral groove" and note the variable degree to which such grooves are developed in different species and/or ontogenetic stages (Raven, 1937; Besharse, 1971). Even in skulls of physically mature individuals, where the basirostral groove is well ossified and obscure, it is still possible to discern its general location based on the occurrence of small, randomly spaced foramina along its broadly curvilinear length. Clearly, the ziphiid basirostral groove is homologous with the dental alveoli of toothed cetaceans (including aetiocetids) and the open alveolar groove of fetal, edentulous mysticetes. However, the position of the basirostral groove on the extreme lateral margin of the rostrum and the lack of associated, well-defined sulci indicate that the ziphiid condition is not homologous with the lateral palatal foramina of aetiocetids and edentulous mysticetes. Ziphiids display a

variable vascular pattern on the medial portion of the palate that includes bilaterally symmetrical pairs of palatine foramina, commonly with long sulci.

Among members of Physeteridae, an "alveolar sulcus" occurs on the anterior half of each maxilla in *Kogia*, and a "strongly marked groove" (the "dental groove") is present on the middle portion of each maxilla in *Physeter* (Flower, 1869; Schulte, 1917; Deméré personal observation). In both cases, the longitudinal sulcus is positioned roughly midway between the medial and lateral margins of the maxilla. In *Kogia*, the alveolar sulcus is continuous posteriorly with a canal within the maxillary that presumably transmits the alveolar artery and nerve to the rudimentary dentition. Anteriorly, the alveolar sulcus extends to the tip of the maxilla. Importantly, there are no individual lateral foramina and no associated sulci. In *Physeter*, the condition is similar to *Kogia*, but with an open dental groove extending for a greater distance along the maxilla. The exposed length of this groove is variable and in some individuals is roofed over to form a concealed canal. As in *Kogia*, there are no lateral foramina with associated sulci.

Presence of SCPP Dental Genes in Edentulous Mysticetes

We attempted to PCR amplify and sequence segments of four SCPP exons from 13 mysticete species. In 12 of the 13 taxa, all four exons amplified, and PCR products were of expected length. *Eubalaena glacialis* (North Atlantic right whale; Northeast Fisheries Science Center [SWFCS] no. Z13086) was the exception. *ENAM* did not amplify for this species, possibly because *ENAM* or part of this gene has been deleted from the *E. glacialis* genome. Amplification using primers 3′ to the region analyzed here also failed to yield *ENAM* sequence from *E. glacialis*.

Phylogenetic Hypotheses (Mysticete Supermatrix)

Parsimony analyses of the supermatrix produced a well-resolved phylogenetic hypothesis for Mysticeti (Figs. 3 to 5). With all characters unordered, there were 82 optimal trees with minimum length of 11,967 steps (retention index [Farris, 1989] = 0.491); ordering a subset of characters (Appendix 2) resulted in six minimum length trees (11,998 steps; retention index = 0.495) and gave slightly more resolution than the unordered analysis (Fig. 3). Examination of all most parsimonious cladograms showed that relationships among extant mysticetes were generally congruent with recent molecular studies (Árnason et al., 2004; Rychel et al., 2004; Sasaki et al., 2005, 2006; Nikaido et al., 2006). *Eschrichtius robustus* (gray whale, Eschrichtiidae) was placed as the extant sister species to *Balaenoptera* spp. + *Megaptera novaeangliae* (rorquals, Balaenopteridae). *Caperea marginata* (pygmy right whale, Neobalaenidae) and *Eubalaena* + *Balaena mysticetus* (right and bowhead whales, Balaenidae) were successive sister taxa to the Eschrichtiidae + Balaenopteridae clade (Fig. 4). Relationships among extant lineages were obscured by the instability of some extinct taxa (Fig. 3), but when fossils were excluded from analysis, solid support for extant clades was revealed (Fig. 4).

The basic branching sequence among fossil stem mysticetes was consistently supported by analyses of the supermatrix and the morphological data alone regardless of whether characters were unordered or ordered (Fig. 4; clades A to E; support scores shown in Fig. 3). Because stem mysticetes were not coded for molecular data, all unequivocally optimized synapomorphies at basal nodes of the supermatrix tree were changes in skeletal and dental characters. Among edentulous taxa, crown mysticetes (the last common ancestor of extant baleen whales and all of its descendants) grouped with "cetotheres" (clade A; Bremer +2 to +5; bootstrap 87% to 95%). All "cetothere" genera sampled here (*Cetotherium, Mixocetus, Cophocetus, Isanacetus, Parietobalaena, Pelocetus, Aglaocetus, Diorocetus*) were excluded from crown group Mysticeti as in several recent cladistic analyses (Geisler and Sanders, 2003; Deméré et al., 2005; Bouetel and Muizon, 2006; Fitzgerald, 2006). In contrast to these studies and others (Kimura and Ozawa, 2002; Bisconti, 2007; Steeman, 2007), a monophyletic "Cetotheriidae" was weakly supported (Fig. 3). Six morphological characters that showed no homoplasy on minimum length trees substantiated the monophyly of all edentulous mysticetes (clade B; Bremer +10 to +11; bootstrap 99%), and a sister group relationship between *Eomysticetus whitmorei* from the Late Oligocene (~28 Ma) and the remaining toothless taxa was resolved (Figs. 3, 4).

All optimal topologies suggest that Late Oligocene toothed mysticetes (*Aetiocetus weltoni*, *A. cotylalveus*, *A. polydentatus*, *Chonecetus goedertorum*, *Mammalodon colliveri*, *Janjucetus hunderi*) represent ancient lineages (Figs. 3, 4); Aetiocetidae, Mammalodontidae, and Janjucetidae were placed as successive sister groups to edentulous mysticetes (clades C to E). The toothless forms grouped with Aetiocetidae (*Aetiocetus* + *Chonecetus*) to the exclusion of other taxa in the analysis (clade C; Bremer +1; bootstrap <50% to 50%). Monophyly of Aetiocetidae (Bremer +2 to +3; bootstrap 78% to 83%) agreed with the analyses of Geisler and Sanders (2003), Kimura and Ozawa (2002), Bisconti (2007), and Steeman (2007) but conflicted with recent hypotheses that favored aetiocetid paraphyly (Bouetel and Muizon, 2006; Fitzgerald, 2006). *Mammalodon colliveri* (Mammalodontidae) clustered as the sister group to clade C, and this grouping, clade D, was weakly supported (Fig. 3). Three unique and unreversed morphological synapomorphies substantiated monophyly of Mysticeti (clade E; Bremer +2 to +3; bootstrap 73% to 93%), with a basal split between *Janjucetus hunderi* (Janjucetidae) and all other mysticetes.

Separate analysis of the morphological data corroborated the branching sequence at the base of the supermatrix tree (Fig. 3). The phenotypic data supported clades A to E (Fig. 4) as well as Odontoceti, Aetiocetidae, Balaenidae, Balaenopteridae, and Balaenopteridae + Eschrichtiidae. A grouping of "cetotheres" and crown mysticetes was retained (clade A), but "Cetotheriidae" was

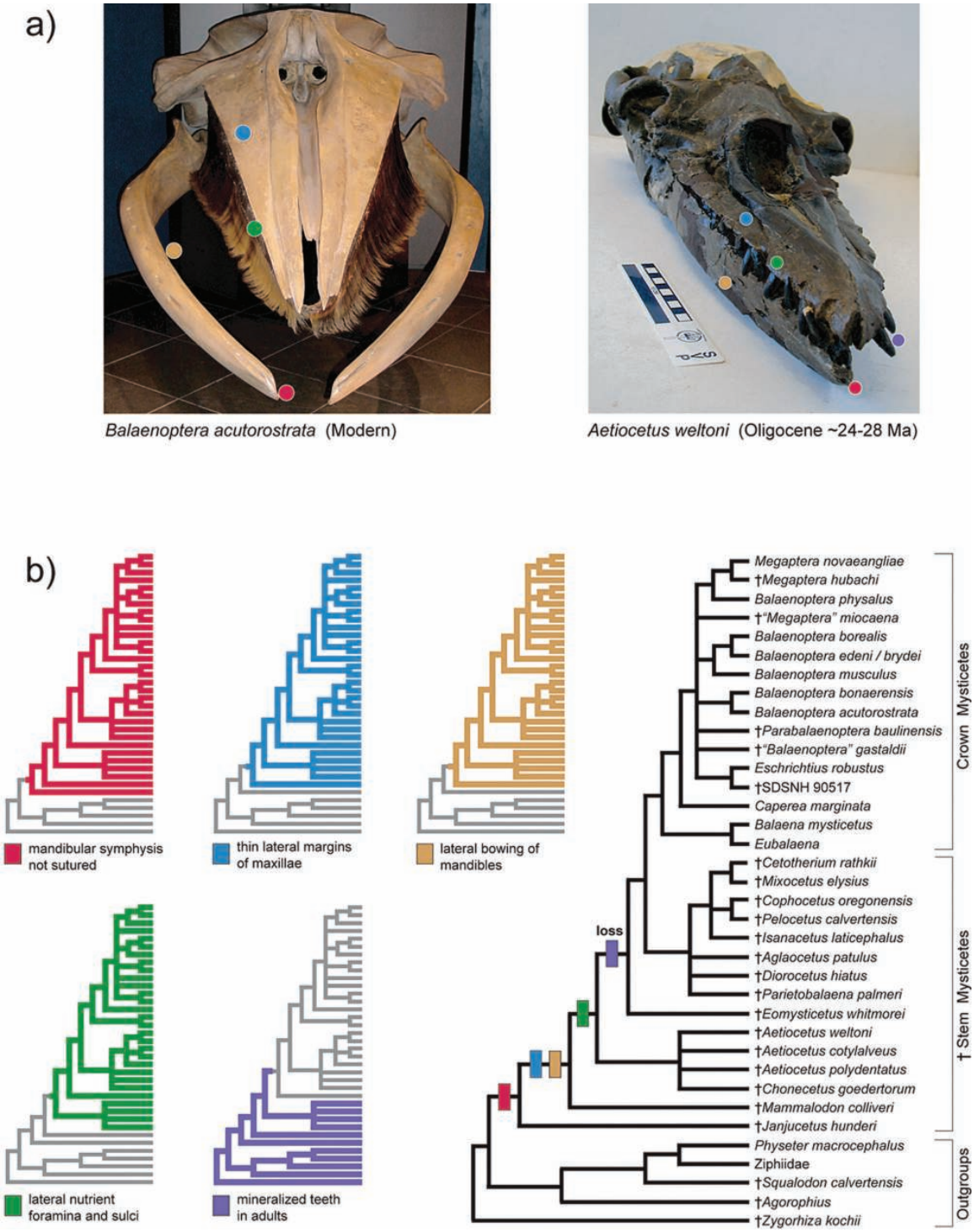

FIGURE 5. Loss of mineralized teeth in Mysticeti after the evolution of lateral nutrient foramina and other features linked to bulk filter-feeding using baleen. (a) Anterior view of skull, mandibles, and baleen apparatus of extant edentulous mysticete (*Balaenoptera acutorostrata*; National Science Museum, Tokyo) and anterolateral view of skull and mandibles of fossil toothed mysticete (*Aetiocetus weltoni*; UCMP 122900) showing the distribution of five character states: unsutured mandibular symphysis (red; character no. 53), thin lateral margins of maxillae (blue; no. 4), lateral bowing of mandibles (yellow; no. 57), lateral nutrient foramina and sulci (green; no. 38; see Fig. 1), and mineralized teeth in adults (purple; no. 61). Relative to outgroups, the ramus of the mandible is laterally bowed in *A. weltoni*; this lateral curvature is further accentuated in some edentulous taxa, such as *B. acutorostrata*. (b) Parsimony optimizations of these five characters on a phylogenetic hypothesis for 31 mysticetes and five outgroup taxa (Fig. 3) are shown to the left; the sequence of inferred character state changes is shown to the right. The presence of a relatively broad rostrum (character no. 2) also was unequivocally optimized to the last common ancestor of Mysticeti, but there were several reversals to a narrower condition in the group.

paraphyletic, and in some minimum length trees was placed within crown Mysticeti (see Kimura and Ozawa, 2002; Bisconti, 2005, 2007; Steeman, 2007). Among extant taxa, the morphological data favored a grouping of Neobalaenidae with Balaenidae, a result that has been uniformly and robustly supported by recent morphological analyses (Geisler and Sanders, 2003; Bisconti, 2005, 2007; Deméré et al., 2005; Bouetel and Muizon, 2006; Fitzgerald, 2006; Steeman, 2007). This clade, Balaenoidea, represents the strongest incongruence between the morphological evidence and our supermatrix results but did not influence the interpretation of critical character state changes at the base of the mysticete tree.

Analyses of individual molecular data sets generally did not strongly contradict relationships among exant mysticete species supported by the supermatrix (Fig. 4). The common cetacean satellite sequence (Árnason et al., 1992) was the only molecular partition that showed ≥95% bootstrap support for a clade that conflicted with the supermatrix results. The satellite sequences robustly grouped *Balaenoptera physalus* with *Balaenoptera musculus* to the exclusion of *Megaptera novaeangliae* (Árnason et al., 1992). Regardless, the same minimum length topologies were supported whether the satellite sequences were included or excluded from the supermatrix, demonstrating the stability of the overall result.

Phylogenetic Hypotheses (Dental Gene Matrix)

Parsimony and Bayesian analyses of the three SCPP dental genes gave congruent results. There were three minimum length topologies (1967 steps; retention index = 0.738), and one of these was identical to the Bayesian majority-rule consensus (Fig. 6a). Relationships among outgroups to Mysticeti generally were consistent with recent supermatrix analyses of Cetartiodactyla (Gatesy et al., 1999, 2002). Delphinida, Odontoceti, Mysticeti, Cetacea, Cetacea + Hippopotamidae, Bovidae, Pecora, Ruminantia, Cetruminantia, Suina, Camelidae, Cetartiodactyla, and Cetartiodactyla + Perissodactyla were supported by all analyses (Fig. 6). Within Mysticeti, several clades supported by the dental gene data also were corroborated by the supermatrix analyses; these included Balaenidae, *Megaptera novaeangliae* + *Balaenoptera physalus*, *B. borealis* + *B. edeni*/*B. brydei*, and *M. novaeangliae* + *B. physalus* + *B. borealis* + *B. edeni*/*B. brydei* + *B. musculus*. However, there was evidence for inconsistent sorting of ancestral polymorphism in *ENAM*, the gene that encodes enamelin. In particular, two adjacent gap characters in *ENAM* supported an unconventional grouping of *Eschrichtius robustus*, *Caperea marginata*, *Balaenoptera acutorostrata*, and *Balaenoptera bonaerensis* (Fig. 6a); this group, which has never been proposed previously, was supported by Bayesian analysis of the dental gene matrix and by one of the minimum length trees for this data set. *ENAM* was amplified from additional individuals of *Caperea marginata* and *Eschrichtius robustus* to ensure that this result was not due to PCR contamination, and the new sequences matched those from conspecifics (Fig. 6a). Similar evidence for deep coalescence, or perhaps introgression, was reported in a recent analysis of transposon insertions in Mysticeti (Nikaido et al., 2006).

Character Mapping

Because basal relationships in the mysticete tree were consistent across analyses (Figs. 3, 4), the evolutionary loss of mineralized teeth in adults and the evolutionary gain of lateral nutrient foramina were unequivocally mapped on all trees supported by the supermatrix. The derivation of lateral nutrient foramina (character no. 38) preceded the loss of teeth (no. 61), and aetiocetid mysticetes documented the mosaic, intermediate condition in this transformation (Fig. 5). In addition to lateral nutrient foramina on the palate, the common ancestor of Aetiocetidae and all toothless mysticetes (Fig. 4, clade C) was characterized by a relatively broad rostrum (no. 2), an unsutured mandibular symphysis (no. 53), thin lateral margins of maxillae (no. 4), and incipient lateral bowing of the mandibles (no. 57). Parsimony optimizations imply that the latter four characters were derived before the acquisition of nutrient foramina (Fig. 5); these four traits suggest an expansion in volume of the oral cavity and may designate the initial shift to a filter-feeding strategy in Mysticeti.

We also mapped molecular changes in three SCPP dental genes onto two phylogenetic hypotheses for Mysticeti and outgroups (Fig. 6). Translation of SCPP DNA sequences in all three reading frames revealed premature stop codons in the enamel-specific genes of baleen whales. Alignment of mysticete sequences to outgroup sequences showed that the premature stop codons were due to single base pair indels in the *AMBN* and *ENAM* genes of various mysticete species (Fig. 6) and one nonsense substitution in the *AMBN* sequence of *Balaenoptera bonaerensis* (a change from TAC [tyrosine] to TAA [stop]). Parsimony optimizations of indel characters onto the two alternative topologies showed the same basic pattern. There was very little homoplasy in the indel character set (consistency index = 0.875–0.913; retention index = 0.895–0.930). Outside of Mysticeti, all indels were multiples of three base pairs (minimally 37 indels for each tree). Within Mysticeti, indels were predominantly frameshift mutations in enamel-specific genes that resulted in premature stop codons (minimally 7 to 8 frameshifts and 2 to 3 indels in multiples of three basepairs). All parsimony reconstructions implied that these frameshift indels occurred subsequent to evolutionary loss of the mineralized dentition in baleen whales. For the regions of *AMBN* and *ENAM* that we sequenced, no frameshifts were mapped to the common ancestor of all extant mysticetes (Fig. 6).

DISCUSSION

Loss of the Dentition and Inactivation of Enamel-Specific Genes

The supermatrix for Mysticeti includes mt genomes, data from 17 nuclear DNA markers, insertions of transposons, and morphological characters; by compiling new and published data, the goal was to discern common

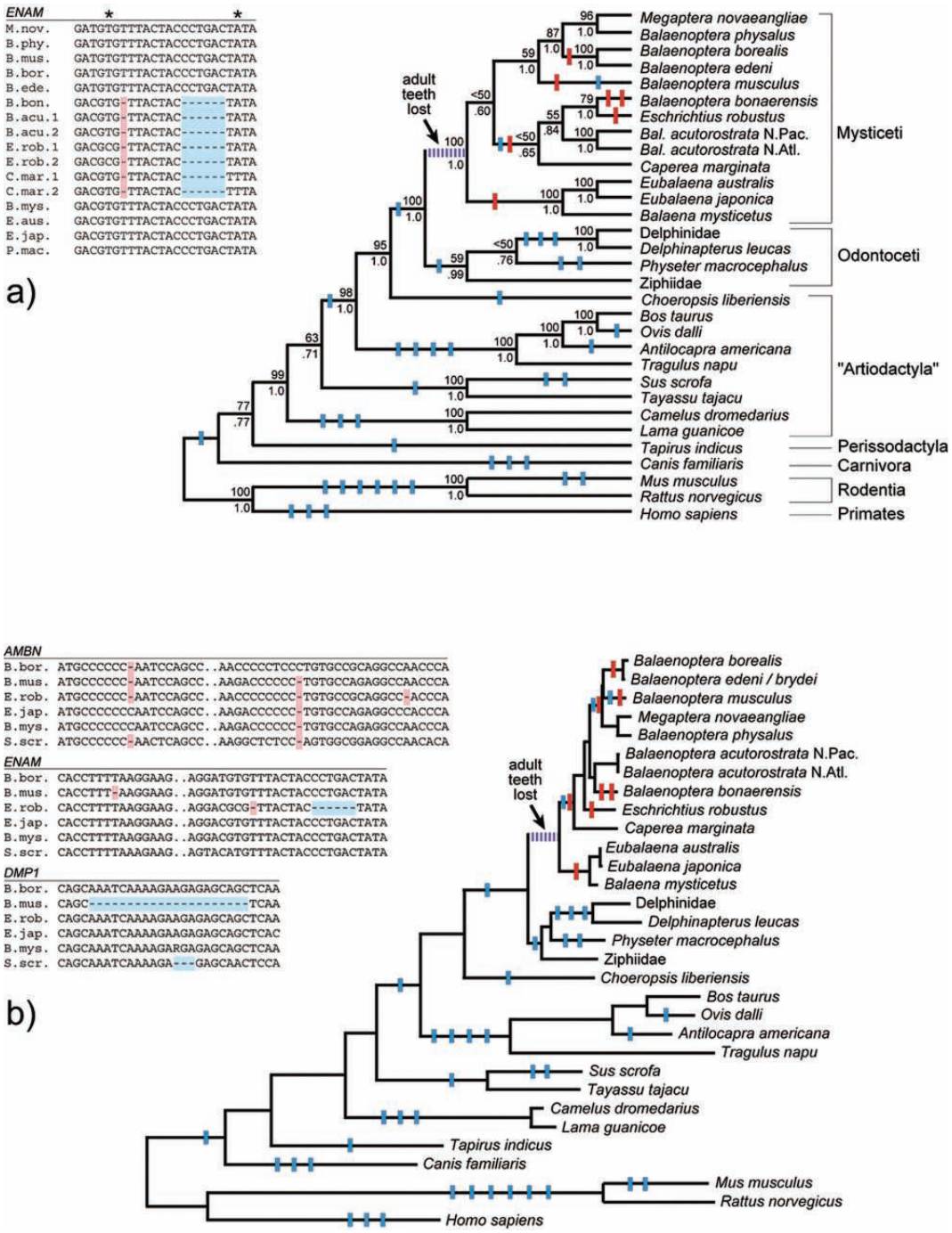

FIGURE 6. Length mutations in *AMBN*, *ENAM*, and *DMP1* mapped onto phylogenetic hypotheses for edentulous mysticetes and toothed outgroups. The trees and alignments show inferred indel events (red = frameshift mutation; blue = indel in multiple of three base pairs). Frameshift mutations that cause premature stop codons are present in Mysticeti but absent from Odontoceti and more distant mammalian outgroups. All frameshifts were restricted to enamel-specific SCPP genes and occurred after loss of the mineralized adult dentition on the stem lineage of Mysticeti (dashed purple lines; also see Fig. 5b). (a) Bayesian consensus tree that is identical to one of the minimum length cladograms for the dental gene matrix. Numbers at internodes show parsimony bootstrap percentage (top) and Bayesian posterior probability (bottom). "<50" indicates a bootstrap score <50% and marks clades that collapse in the strict consensus of three minimum length topologies. The inset shows a frameshift deletion of one base and a deletion of six bases in the sequence alignment for *ENAM*. Asterisks identify positions of the *ENAM* alignment where there are species-specific substitutions in *Caperea marginata* and *Eschrichtius robustus*. (b) Composite topology with relationships among mysticetes following the supermatrix analysis (Fig. 4) and relationships among outgroups based on Bayesian analysis of the three dental genes. Aligned nucleotide sequences for five mysticetes and domestic pig (*Sus scrofa*) illustrate representative indels in the SCPP dental genes. ".." indicates sections of sequence omitted to save space. Parsimony branch lengths are proportional to the numbers of substitutions in the three SCPP genes. Taxon abbreviations in the sequence alignments are first letter of genus name followed by first three letters of species name.

phylogenetic signals from diverse characters (Kluge, 1989). Parsimony analyses of the supermatrix and of the phenotypic data alone supported trees with a consistent branching sequence at the base of Mysticeti (Figs. 3 to 5). Given the phylogenetic position of the archaic toothless mysticete, *Eomysticetus whitmorei* (Late Oligocene), and the parsimony optimization of character no. 61 (presence/absence of mineralized teeth in adults), the evolutionary loss of teeth occurred prior to the first appearance of this edentulous species, ~28 Ma (Sanders and Barnes, 2002a). This ancient transformation (Fig. 5b) marks the time when tooth-aided predation was no longer an option for the direct ancestors of extant mysticetes and when the dentition was relegated to its present rudimentary condition (Fig. 1c).

A survey of SCPP genes yielded compelling evidence for a release from selective constraints on enamel-specific genes with the loss of functional teeth. Insertions and deletions in *AMBN*, *ENAM*, and *DMP1* were mapped onto phylogenetic hypotheses (Fig. 6). For Odontoceti and other toothed outgroups to Mysticeti, all inferred indel events were multiples of three nucleotides and did not disrupt the reading frames of the dental genes. By contrast, within Mysticeti, ~70% of indels were frameshift mutations restricted to *AMBN* and *ENAM*, enamel genes expressed primarily by secretory ameloblasts. There were no frameshift mutations in the multi-functional *DMP1* gene. Premature stop codons in *AMBN* and *ENAM* of baleen whales suggest that these loci are decaying pseudogenes. Thus, extant mysticetes retain both developmental (Fig. 1c) and genetic (Fig. 6) evidence of their ancestral toothed heritage (Figs. 1, 2, and 5); vestigial genes that previously encoded enamel-specific proteins represent "molecular fossils" in the genomes of modern baleen whales.

Early Evolution of Nutrient Foramina and Baleen

We discovered a series of eight well-preserved nutrient foramina and associated sulci on the lateral portion of the palate of *Aetiocetus weltoni*, a Late Oligocene toothed mysticete (Figs. 1, 2; Deméré, 2005). Similar features also were found in two additional aetiocetid species, *Aetiocetus cotylalveus* and *Chonecetus goedertorum*, and a recent meeting abstract suggests that nutrient foramina may be present in a fourth species (Sawamura et al., 2006). To our knowledge, such foramina and sulci are absent in all cetaceans except edentulous mysticetes and, based on their anatomical position and orientation in the aetiocetids, were coded as homologues to the nutrient foramina of modern baleen whales. Nearly parallel, parasagittal sulci on the anterior portion of the palate are shared by *A. weltoni* and all extant mysticete genera, but palatal vascularization in *A. weltoni* is overall most reminiscent of that in extant rorquals (Fig. 1a, b). Given our best-supported phylogenetic hypotheses (Figs. 3, 4), this similarity implies that an approximation of the balaenopterid condition is the primitive state and that the arrangement of foramina/sulci on the posterolateral palate has diverged in other extant mysticete clades.

Parsimony reconstructions of ancestral character states indicated that lateral nutrient foramina evolved in the common ancestor of aetiocetids and edentulous mysticetes, >28 Ma (Figs. 4, 5). The nutrient foramina and associated sulci are thought to serve the same basic function in all extant baleen whales; these passages house blood vessels and nerves that nourish and innervate the baleen-producing epithelia of the mysticete palate (Walmsley, 1938). In turn, the primary function of baleen in extant species is to strain groups of small prey items from seawater (Pivorunas, 1979). Therefore, in the context of our phylogenetic analyses (Figs. 3, 4), the simplest interpretation of the available evidence is that toothed mysticetes with lateral nutrient foramina expressed baleen (Fig. 7), and that the function of this early baleen was to filter minute prey. Other explanations would require additional evolutionary changes in function and would be less parsimonious given the current state of knowledge.

Lateral nutrient foramina in aetiocetids imply the presence of baleen, but the specific morphology of this early baleen system cannot be determined with confidence from the arrangement of foramina and sulci on the palate. The baleen racks of extant mysticetes include main plates, minor plates, and "hairs" (Williamson, 1973). Individual plates consist of a central medulla layer of keratinous tubules that are cemented together and sandwiched between smooth outer cortical layers of keratin, whereas hairs are composed of single keratinous tubules (Utrecht, 1965). Given this spectrum in complexity, the baleen of *Aetiocetus* may have been simply arranged, perhaps as small bundles of keratinous tubules (Fig. 7). Such bundles occur at the front and rear of the baleen racks in modern balaenopterids (Williamson, 1973), and in *Aetiocetus* could have formed a primitive filter between the widely spaced teeth of the upper dentition (Fig. 2) when in near occlusion with the interdigitating lower dentition (Fig. 5a).

Stepwise Transition from Teeth to Baleen in Mysticeti

Based solely on observations of extant taxa, the transition from tooth-aided predation to filter-feeding with baleen would seem a daunting macroevolutionary hurdle. For example, extant balaenopterids utilize an integrated suite of behavioral and anatomical specializations to feed on aggregations of zooplankton and small fish (Werth, 2000). Lunge feeding in *Balaenoptera musculus* (blue whale) has been described as the world's largest biomechanical event (Croll and Tershy, 2002); >70 tons of water may be engulfed and then expelled through the baleen filter in one feeding episode (Pivorunas, 1979). To routinely process these huge volumes, the balaenopterid skull has been radically reorganized in comparison to extant odontocete cetaceans. Modified jaw articulations, a broad rostrum, bowed dentaries, a ligamentous mandibular symphysis, the frontomandibular stay system, cranial and rostral kinesis, a highly elastic throat pouch that is pleated externally, and the baleen filtering apparatus work in concert and permit the bulk capture of

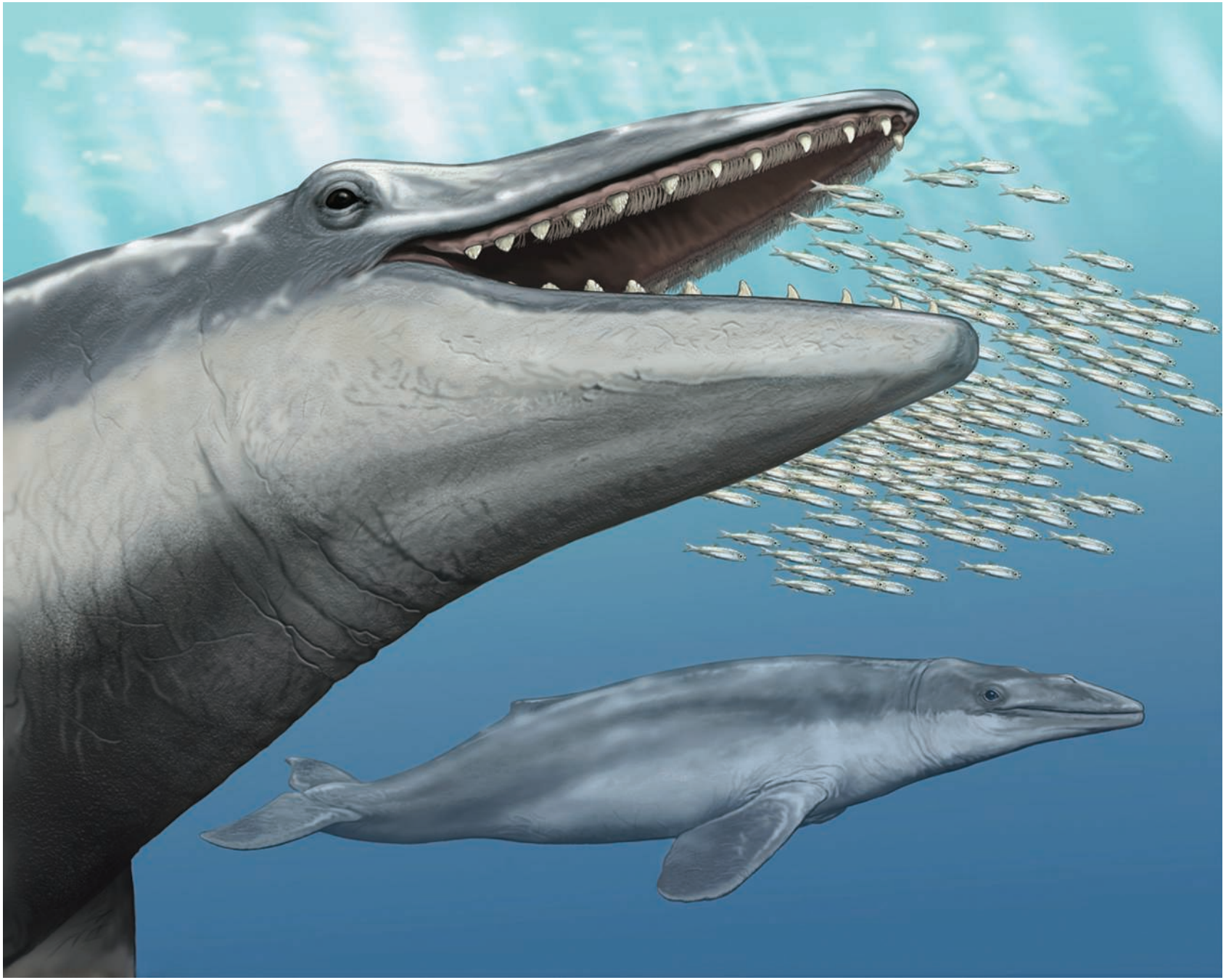

FIGURE 7. Reconstruction of *Aetiocetus weltoni*, showing hypothesized simultaneous occurrence of teeth and baleen (painting by Carl Buell).

entire schools of prey (Pivorunas, 1977, 1979; Orton and Brodie, 1987; Lambertsen, 1983; Lambertsen et al., 1995; Werth, 2000; Croll and Tershy, 2002). Baleen whales that continuously skim prey from the water column (*Balaena* and *Eubalaena*) or suction-feed on benthic invertebrates (*Eschrichtius*) possess comparably elaborate anatomical modifications (Pivorunas, 1979; Werth, 2000, 2004; Bouetel, 2005). All extant mysticetes have highly derived feeding anatomies relative to odontocetes and more distant "archaeocete" outgroups.

The fossil record also shows a gap in anatomy between toothed and toothless mysticetes. Most recent phylogenetic analyses of Mysticeti imply an evolutionary jump from a primitive form with tooth-lined jaws and no baleen to the modern condition where the jaws are toothless and racks of baleen plates are suspended from the palate (Kimura and Ozawa, 2002; Sanders and Barnes, 2002a; Geisler and Sanders, 2003; Bisconti, 2005, 2007; Bouetel and Muizon, 2006; Steeman, 2007; but see Fitzgerald, 2006). The discovery of lateral nutrient foramina in toothed aetiocetid mysticetes reveals a stepwise evolutionary solution to traversing this gap in feeding anatomy (Fig. 5). *Aetiocetus weltoni* and other Oligocene aetiocetids are mosaic taxa in which both ancestral and descendant feeding morphologies are expressed. Specifically, a full dentition (the primitive state) might have been used to capture individual prey (wear facets suggest that the teeth were functional), and incipient baleen (the derived state) could have been employed to batch-filter smaller prey items (Fig. 7). Because ancestral feeding structures were retained, the subsequent evolution of baleen may have broadened the range of prey that early mysticetes exploited. The complex of traits that characterize derived filter-feeders could evolve gradually because ancestral feeding structures were not abandoned prematurely (Fig. 5b). Published phylogenetic trees conflict in detail with our overall systematic hypothesis (Kimura and Ozawa, 2002; Sanders and Barnes, 2002a; Geisler and Sanders, 2003; Bisconti, 2005, 2007; Bouetel and Muizon, 2006; Fitzgerald, 2006; Steeman, 2007), but given the presence of lateral nutrient foramina in aetiocetids, parsimony optimizations consistently show that baleen evolved before the loss of teeth in all of these alternative topologies.

The derivation of baleen might mark the initial transition to filter-feeding in Mysticeti or may simply represent an incremental improvement in the primitive filter-feeding apparatus of early toothed mysticetes. Prior to the discovery of lateral nutrient foramina in aetiocetids, several authors suggested that toothed mysticetes filtered small prey with their teeth (Fordyce, 1984, 1989; Mitchell, 1989; Fordyce and Barnes, 1994; Barnes et al., 1995; Ichishima, 2005), as in extant crabeater seals (Klages and Cockroft, 1990). It is possible that the evolution of baleen enabled more efficient bulk feeding on organisms that would have otherwise escaped a relatively crude dental sieve. Numerous anatomical specializations allow extant mysticetes to process a large volume of water in the mouth and facilitate filter-feeding with baleen (Pivorunas, 1977; Fordyce, 1982; Lambertsen, 1983; Barnes et al., 1995; Bouetel, 2005; Fitzgerald, 2006). Among characters that fossilize, parsimony reconstructions imply that a broadened rostrum, an unsutured mandibular symphysis, thin lateral margins of maxillae, and lateral bowing of the mandibles evolved at basal nodes in the mysticete clade, before the evolution of nutrient foramina and subsequent loss of the dentition (Fig. 5). This sequence suggests that the transition to filter-feeding may have occurred before the evolution of baleen or, alternatively, that characters utilized by modern baleen whales for filter-feeding initially were recruited for alternative functions (see discussion in Fordyce, 1982; 2003b; Barnes et al., 1995; Bouetel, 2005; Fitzgerald, 2006).

A stepwise pattern of macroevolution apparently is rare but has been documented previously at both the morphological and behavioral levels of organization. For example, the respiratory apparatus of amniotes is the result of a stepped transformation (Liem, 1988) that included change from gills (primitive state), to gills and lungs (intermediate state), to only lungs present (derived state). The mosaic intermediate condition is still found in extant species (e.g., lungfishes). At the behavioral level, de Queiroz (2003) suggested that in *Thamnophis* (garter snakes) a transition in feeding behavior included change from tactile aquatic feeding (primitive state), to both tactile and visual aquatic feeding (intermediate state), to visual aquatic feeding (derived state). All three behavioral repertoires are seen in closely related extant species (de Queiroz, 2003). Analogous patterns may occur at the molecular level; gene duplication, divergence, and pseudogenization (Zhang, 2003) might be expected to generate a stepwise pattern of evolution in some cases.

Future Tests of Phylogenetic Patterns and Evolutionary Scenarios

Given our phylogenetic results (Figs. 3 to 5), we hypothesize that aetiocetid mysticetes had a mosaic phenotype in which both teeth and baleen were present in adults (Fig. 7). Furthermore, we suggest that by extending the size range of prey that could be captured efficiently, the composite feeding anatomy of aetiocetids may have facilitated the transition from ancestral toothed forms to derived filter-feeders that are toothless. These inferences can be tested by future paleontological discoveries and by extending analysis of the current database. At the most basic level, fossilized baleen from aetiocetids would provide definitive evidence for the joint expression of teeth and baleen and might reveal the structure and extent of the early baleen filter. Although rare, fossil baleen has been reported from several Neogene deposits around the Pacific (Pilleri and Pilleri, 1989; Goodwin and Barnes, 2003), and additional but undescribed examples are represented in museums in North America, Japan, and Europe.

Several lines of evidence potentially offer insights on the feeding ecology of toothed mysticetes. Well-preserved stomach contents would document the size range and taxonomic representation of ingested prey.

Fossilized stomach contents from Eocene whales suggest that some "archaeocetes" (*Basilosaurus* and *Dorudon*) consumed fish (Swift and Barnes, 1996; Uhen, 2004), but data from Aetiocetidae currently are lacking. Examination of shear facets and other dental wear also could generate clues regarding the dietary preferences of toothed mysticetes (Fitzgerald, 2006), and the chemical compositions of mineralized tissues provide independent evidence of paleo-diet. Clementz et al. (2006) recently suggested that comparisons of calcium isotope ratios might help characterize the shift to filter-feeding in stem mysticetes by discriminating species that fed at lower versus higher trophic levels.

In terms of systematic analysis, inclusion of additional taxa with unique combinations of characters will provide more complete hypotheses of phylogenetic history and a broader framework for reconstructing the order and timing of evolutionary events. *Eomysticetus whitmorei*, an edentulous species, was the geologically oldest mysticete in our phylogenetic analysis (Figs. 3, 4); however, several undescribed fossils are thought to represent ancient toothed mysticete lineages (Barnes and Sanders, 1996; Fordyce, 2003a; Sawamura et al., 2006). In particular, *Llanocetus denticrenatus* (Llanocetidae) dates to near the Oligocene/Eocene boundary (Fordyce, 2003a). Formal description and comparative study of this and other recently discovered fossils will be required to further clarify the branching pattern at the base of Mysticeti and the sequential evolution of feeding anatomy in this group.

Conclusion

The origin of filter-feeding in Mysticeti represents a major ecological shift in mammalian evolution that permitted the exploitation of vast, underutilized prey resources. A broad synthesis of embryological observations, DNA sequences, and paleontological data yields a coherent reconstruction of mysticete phylogeny. The stepwise evolutionary transformation from an archaic toothed condition, to an intermediate state with both teeth and baleen (Fig. 7), to the derived state with only baleen in adults, mirrors the ontogenetic trajectory in extant mysticetes. The end product of this evolutionary sequence is modern filter-feeding baleen whales that have degenerate enamel pseudogenes and rudimentary teeth that are resorbed before birth. These heirlooms from ancient toothed ancestors, in combination with new fossil evidence, provide a multifaceted record of a fundamental macroevolutionary transition in Mysticeti.

Acknowledgments

P. Holroyd and UCMP allowed preparation and study of UCMP 122900. R. Clark prepared the skull of UCMP 122900. D. Archibald, N. Ayoub, C. Buell, M. Collin, R. Debry, J. Garb, S. Gatesy, C. Hayashi, J. Mead, A. de Queiroz, S. Steppan, A. Summers, and an anonymous reviewer discussed and improved the work. T. Gunther, K. Kalkat, H. Lee, S. Lee, K. Randall, A. Rychel, and M. Spaulding provided technical assistance. Southwest Fisheries Science Center–Genetics Archive (LaJolla, CA), the New York Zoological Society (Bronx, NY), South Australian Museum (Adelaide, Australia), the Marine Mammal Center (Sausalito, CA), North Slope Borough (Barrow, AK), Northeast Fisheries Science Center–Stranding Network (Woods Hole, MA), G. Amato, U. Árnason, S. Chivers, M. Cronin, A. Dizon, S. Donnellan, M. Milinkovitch, P. Morin, K. Robertson, and H. Rosenbaum donated DNA samples. Ú. Árnason provided common cetacean satellite sequences. L. G. Barnes, D. Bohaska, and H. Sawamura provided access to fossil specimens. Funding was from NSF DEB-0213171 (JG), DEB-0212572 (JG), DEB-0212238 (TD), and DEB-0212248 (AB). Contributions of the authors: TD and AB discovered nutrient foramina in aetiocetid mysticetes and described the palatal anatomy of *Aetiocetus weltoni*. TD, AB, and MM compiled the morphological data. JG generated the new DNA sequence data. JG and MM compiled the molecular data and executed the phylogenetic analyses. All authors discussed the results and were involved in writing the paper.

References

Árnason, Ú., S. Grétarsdóttir, and B. Widegren. 1992. Mysticete (baleen whale) relationships based upon the sequence of the common cetacean DNA satellite. Mol. Biol. Evol. 9:1018–1028.

Árnason, Ú., A. Gullberg, and A. Janke. 2004. Mitogenomic analyses provide new insights into cetacean origin and evolution. Gene 333:27–34.

Arnold, P. W., R. A. Birtles, A. Dunstan, V. Lukoschek, and M. Matthews. 2005a. Colour patterns of the dwarf minke whale *Balaenoptera acutorostrata* sensu lato: description, cladistic analysis and taxonomic implications. Mem. Queensland Mus. 51:277–307.

Arnold, P. W., R. A. Birtles, S. Sobtzick, M. Matthews, and A. Dunstan. 2005b. Gulping behaviour in rorqual whales: Underwater observations and functional interpretation. Mem. Queensland Mus. 51:309–332.

Barnes, L. G. 1990. The fossil record and evolutionary relationships of the genus *Tursiops*. Pages 3–26 *in* The bottlenose dolphin (S. Leatherwood and R.R. Reeves, eds.). Academic, New York.

Barnes, L. G., and S. McLeod. 1984. The fossil record and phyletic relationships of gray whales. Pages 3–32 *in* The gray whale *Eschrichtius robustus* (M. L. Jones, S. L. Swartz, and S. Leatherwood, eds.). Academic, New York.

Barnes, L. G., M. Kimura, H. Furusawa, and H. Sawamura. 1995. Classification and distribution of Oligocene Aetiocetidae (Mammalia; Cetacea; Mysticeti) from western North America and Japan. Island Arc 3:392–431.

Barnes, L. G., and A. E. Sanders. 1996. The transition from archaeocetes to mysticetes: Late Oligocene toothed mysticetes from near Charleston, South Carolina. 6th NAPC Abstracts, Paleo. Soc. Spec. Publ. 8:24.

Besharse, J. C. 1971. Maturity and sexual dimorphism in the skull, mandible, and teeth of the beaked whale *Mesoplodon densirostris*. J. Mamm. 52:297–315.

Bisconti, M. 2000. New description, character analysis, and preliminary phyletic assessment of two Balaenidae skulls from the Italian Pliocene. Palaeo. Ital. 87:37–66.

Bisconti, M. 2005. Skull morphology and phylogenetic relationships of a new diminutive balaenid from the lower Pliocene of Belgium. Palaeontology 48:793–816.

Bisconti, M. 2007. A new basal balaenopterid whale from the Pliocene of northern Italy. Palaeontology 50:1103–1122.

Bisconti, M., and A. Varola. 2000. Functional hypothesis on an unusual mysticete dentary with double coronoid process from the Miocene of Apulia and its systematic and behavioural implications. Palaeo. Ital. 87:19–35.

Boschma, H. 1938. On the teeth and other particulars of the sperm whale *(Physeter macrocephalus* L.). Temminckia 3:151–278.

Boschma, H. 1950. Maxillary teeth in specimens of *Hyperoodon rostratus* (Müller) and *Mesoplodon grayi* von Haast stranded on the Dutch coast. Proc. K. Ned. Akad. Wet. Ser. C 53:3–14.

Boschma, H. 1951. Rows of small teeth in ziphioid whales. Zool. Mededelingen 31:139–148.

Bouetel, V. 2005. Phylogenetic implications of skull structure and feeding behavior in balaenopterids (Cetacea, Mysticeti). J. Mamm. 86:139–146.

Bouetel, V., and C. Muizon. 2006. The anatomy and relationships of *Piscobalaena nana* (Cetacea, Mysticeti), a Cetotheriidae *s.s.* from the Early Pliocene of Peru. Geodiversitas 28:319–395.

Brandt, J. F. 1873. Untersuchungen über die fossilen und subfossilen cetaceen Europa's. Mém. Acad. Impériale Sci. St. Pétersbourg [7] 20:1–372.

Bremer, K. 1994. Branch support and tree stability. Cladistics 10:295–304.

Clementz, M. T., D. Fox, and R. Edwards. 2006. Stable isotope evidence for the evolution of different feeding strategies within the Neoceti. J. Vert. Paleo. 26(Suppl. to 3):51A.

Croll, D. A., and B. R. Tershy. 2002. Filter feeding. Pages 428–432 *in* Encyclopedia of marine mammals (W. Perrin, B. Würsig, and J. Thewissen, eds.). Academic, London.

Deméré, T. A. 1986. The fossil whale, *Balaenoptera davidsonii* (Cope 1872), with a review of other Neogene species of *Balaenoptera* (Cetacea: Mysticeti). Mar. Mamm. Sci. 2:227–298.

Deméré, T. A. 2005. Palate vascularization in an Oligocene toothed mysticete (Cetacea: Mysticeti: Aetiocetidae): Implications for the evolution of baleen. Page 21 *in* Abstracts for the Fourth Triannual Evolution of Aquatic Tetrapods Conference, Akron, Ohio.

Deméré, T. A., A. Berta, and M. R. McGowen. 2005. The taxonomic and evolutionary history of fossil and modern balaenopteroid mysticetes. J. Mamm. Evol. 12:99–143.

Deméré, T. A., M. R. McGowen, A. Berta, and J. Gatesy. 2006. Paleontological and molecular evidence for the transition from teeth to baleen. J. Vert. Paleo. 26(Suppl. to 3):56A.

de Queiroz, A. 2003. Testing an adaptive hypothesis through context-dependence: Effects of water depth on foraging behaviour in three species of garter snakes. Ethology 109:369–384.

Dissel-Scherft, M. C. V., and Vervoort, W. 1954. Development of the teeth in fetal *Balaenoptera physalus* (L.) (Cetacea, Mystacoceti). Proc. K. Ned. Akad. Wet. Ser. C 57:196–210.

Farris, J. S. 1989. The retention index and the rescaled consistency index. Cladistics 5:417–419.

Felsenstein, J. 1985. Confidence limits on phylogenies: An approach using the bootstrap. Evolution 39:783–791.

Feng, J. Q., H. Huang, Y. Lu, L. Ye, Y. Xie, T. W. Tsutsui, T. Kunieda, T. Castranio, G. Scott, L. B. Bonewald, and Y. Mishina. 2003. The dentin matrix protein 1 (dmp1) is specifically expressed in mineralized, but not soft, tissues during development. J. Dent. Res. 82:776–780.

Fitzgerald, E. M. G. 2006. A bizarre new toothed mysticete (Cetacea) from Australia and the early evolution of baleen whales. Proc. R. Soc. B 273:2955–2963.

Flower, W. H. 1869. On the osteology of the cachalot or sperm-whale (*Physeter macrocephalus*). Trans. Zool. Soc. Lond. 6:309–372.

Flower, W. H. 1878. A further contribution to the knowledge of the existing ziphioid whales. genus *Mesoplodon*. Trans. Zool. Soc. Lond. 10:415–437.

Fordyce, R. E. 1981. Systematics of the odontocete whale *Agorophius pygmaeus* and the family Agorophiidae (Mammalia: Cetacea). J. Paleo. 55:1028–1045.

Fordyce, R. E. 1982. A review of Australian fossil Cetacea. Mem. Nat. Mus. Victoria 43:43–58.

Fordyce, R. E. 1984. Evolution and zoogeography of cetaceans in Australia. Pages 929–948 *in* Vertebrate zoogeography and evolution in Australia (M. Archer and G. Clayton, eds.). Hesperion, Perth, Australia.

Fordyce, R. E. 1989. Origins and evolution of Antarctic marine mammals. Spec. Publ. Geol. Soc. Lond. 47:269–281.

Fordyce, R. E. 2003a. Early crown-group Cetacea in the Southern Ocean: The toothed archaic mysticete *Llanocetus*. J. Vert. Paleo. 23(Suppl. 3):50A.

Fordyce, R. E. 2003b. Cetacean evolution and Eocene-Oligocene oceans revisited. Pages 154–170 *in* From greenhouse to icehouse: the marine Eocene-Oligocene transition (D. R. Prothero, L. C. Ivany, and L. Nesbitt, eds.). Columbia University Press, New York.

Fordyce, R. E. 2006. An unexpected diversity of basal baleen whales: Late Oligocene Eomysticetidae from New Zealand. J. Vert. Paleo. 26(Suppl. to 3):62A.

Fordyce, R. E., and L. G. Barnes. 1994. The evolutionary history of whales and dolphins. Annu. Rev. Earth Planet. Sci. 22:419–455.

Fordyce, R. E., and C. Muizon. 2001. Evolutionary history of cetaceans: A review. Pages 169–233 *in* Secondary adaptations of tetrapods to life in water (J.-M. Mazin and V. de Buffrenil, eds.). Verlag Dr. Friedrich Pfeil, Munchen.

Fraser, F. C., and P. E. Purves. 1960. Hearing in cetaceans. Bull. Br. Mus. Nat. Hist. (Zool.) 7:1–140.

Fukumoto, S., T. Kiba, B. Hall, N. Iehara, T. Nakamura, G. Longenecker, P. H. Krebsbach, A. Nanci, A. B. Kulkarni, and Y. Yamada. 2004. Ameloblastin is a cell adhesion molecule required for maintaining the differentiation state of ameloblasts. J. Cell Biol. 167:973–983.

Gaskin, D. E. 1982. The ecology of whales and dolphins. Heinemann, Portsmouth, New Hampshire.

Gatesy, J., and P. Arctander. 2000. Hidden morphological support for the phylogenetic placement of *Pseudoryx nghetinhensis* with bovine bovids: A combined analysis of gross anatomical evidence and DNA sequences from five genes. Syst. Biol. 49:515–538.

Gatesy, J., C. Hayashi, M. Cronin, and P. Arctander. 1996. Evidence from milk casein genes that cetaceans are close relatives of hippopotamid artiodactyls. Mol. Biol. Evol. 13:954–963.

Gatesy, J., C. Matthee, R. DeSalle, and C. Hayashi. 2002. Resolution of a supertree/supermatrix paradox. Syst. Biol. 51:652–664.

Gatesy, J., M. Milinkovitch, V. Waddell, and M. Stanhope. 1999. Stability of cladistic relationships between Cetacea and higher-level artiodactyl taxa. Syst. Biol. 48:6–20.

Geisler, J. H., and Z. Luo. 1996. The petrosal and inner ear of *Herpetocetus* sp. (Mammalia: Cetacea) and their implications for the phylogeny and hearing of archaic mysticetes. J. Paleo. 70:1045–1066.

Geisler, J. H., and A. E. Sanders. 2003. Morphological evidence for the phylogeny of Cetacea. J. Mamm. Evol. 10:23–129.

Gilbert, D. 1992. SeqApp version 1.9a. Bloomington, Indiana.

Gingerich, P. D., M. Haq, I. Zalmout, I. Khan, and M. Malkani. 2001. Origin of whales from early artiodactyls: hands and feet of Eocene Protocetidae from Pakistan. Science 239:2239–2242.

Goodwin, M., and L. G. Barnes. 2003. Carbon isotope analysis and mineralization in fossil and modern mysticete whale baleen plates. J. Vert. Paleo. 23(Suppl. 3):56A.

Hatch, L. T., E. B. Dopman, and R. G. Harrison. 2006. Phylogenetic relationships among the baleen whales based on maternally and paternally inherited characters. Mol. Phylogenet. Evol. 41:12–27.

Heyning, J. E. 1989. Comparative facial anatomy of beaked whales (Ziphiidae) and a systematic revision among the families of extant Odontoceti. Contrib. Sci. Nat. Hist. Mus. Los Angeles Co. 405:1–64.

Hu, J. C.-C., and Y. Yamakoshi. 2003. Enamelin and autosomal-dominant amelogenesis imperfecta. Crit. Rev. Oral Biol. Med. 14:387–398.

Huq, N. L., K. J. Cross, M. Ung, and E. C. Reynolds. 2005. A review of protein structure and gene organisation for proteins associated with mineralised tissue and calcium phosphate stabilisation encoded on human chromosome 4. Arch. Oral Biol. 50:599–609.

Ichishima, H. 2005. Notes on the phyletic relationships of the Aetiocetidae and the feeding ecology of toothed mysticetes. Bull. Ashoro Mus. Paleontol. 3:111–117.

Ishikawa, H., and H. Amasaki. 1995. Development and physiological degradation of tooth buds and development of rudiment of baleen plate in southern minke whale, *Balaenoptera acutorostrata*. J. Vet. Med. Sci. 57:665–670.

Ishikawa, H., H. Amasaki, H. Dohguchi, A. Furuya, and K. Suzuki. 1999. Immunohistological distributions of fibronectin, tenascin, type I, III and IV collagens, and laminin during tooth development and degeneration in fetuses of minke whale, *Balaenoptera acutorostrata*. J. Vet. Med. Sci. 61:227–232.

Karlsen, K. 1962. Development of tooth germs and adjacent structures in the whalebone whale (*Balaenoptera physalus* (L.)). Hvalrådets Skrifter 45:5–56.

Kawasaki, K., T. Suzuki, and K. M. Weiss. 2004. Genetic basis for the evolution of vertebrate mineralized tissue. Proc. Natl. Acad. Sci. USA 101:11356–11361.

Kawasaki, K., and K. M. Weiss. 2003. Mineralized tissue and vertebrate evolution: the secretory calcium-binding phosphoprotein gene cluster. Proc. Natl. Acad. Sci. USA 100:4060–4065.

Kellogg, R. 1923. Description of two squalodonts recently discovered in the Calvert Cliffs, Maryland; and notes on the shark-toothed cetaceans. Proc. U.S. Nat. Mus. 62:1–69.

Kellogg, R. 1934. A new cetothere from the Modelo Formation at Los Angeles, California. Publ. Carnegie Inst. Wash. 447:83–104.
Kellogg, R. 1965. A new whalebone whale from the Miocene Calvert formation. Bull. U.S. Natl. Mus. 247:1–63.
Kellogg, R. 1968a. A hitherto unrecognised Calvert cetothere. Bull. U.S. Natl. Mus. 247:133–161.
Kellogg, R. 1968b. A sharp-nosed cetothere from the Miocene Calvert. Bull. U.S. Natl. Mus. 247:163–173.
Kellogg, R. 1968c. Supplement to description of *Parietobalaena palmeri*. Bull. U.S. Natl. Mus. 247:175–197.
Kim, J.-W., F. Seymen, B. P. -J. Lin, B. Kiziltan, K. Gencay, J. P. Simmer, and J. C. -C Hu. 2005. *ENAM* mutations in autosomal-dominant amelogenesis imperfecta. J. Dent. Res. 84:278–282.
Kimura, T. 2002. Feeding strategy of an Early Miocene cetothere from the Toyama and Akeyo formations, central Japan. Paleo. Res. 6:179–189.
Kimura, T., and T. Ozawa. 2002. A new cetothere (Cetacea: Mysticeti) from the Early Miocene of Japan. J. Vert. Paleo. 22:684–702.
Klages, N. T., and V. G. Cockroft. 1990. Feeding behaviour of a captive crabeater seal. Polar Biol. 10:403–404.
Kluge, A. 1989. A concern for evidence and a phylogenetic hypothesis of relationships among *Epicrates* (Boidae, Serpentes). Syst. Zool. 38:7–25.
Lambertsen, R. H. 1983. Internal mechanism of rorqual feeding. J. Mamm. 64:76–88.
Lambertsen, R. H., N. Ulrich, and J. Straley. 1995. Frontomandibular stay of Balaenopteridae: A mechanism for momentum recapture during feeding. J. Mamm. 76:877–899.
Lee, M. S. Y. 2005. Molecular evidence and marine snake origins. Biol. Lett. 1:227–230.
Levenson, D. H., and A. Dizon. 2003. Genetic evidence for the ancestral loss of short-wavelength-sensitive cone pigments in mysticete and odontocete cetaceans. Proc. R. Soc. Lond. B 270:673–679.
Liem, K. F. 1988. Form and function of lungs: The evolution of air breathing mechanisms. Am. Zool. 28:739–759.
Lindow, B. E. K. 2002. Bardehvalernes indbyrdes slægtskabsforholden foreløbig analyse. Pages 12–19 *in* Resumé-hæfte. Hvaldag 2002 (B.E.K. Lindow, ed.). Midtsønderjyllands Museum, Gram, Denmark.
Luo, Z., and P. D. Gingerich. 1999. Terrestrial Mesonychia to aquatic Cetacea: Transformation of the basicranium and evolution of hearing in whales. Univ. Mich. Pap. Paleo. 31:1–98.
Mårdh, C. K., B. Bäckman, G. Holmgren, J. C.-C. Hu, J. P. Simmer, and K. Forsman-Semb. 2002. A nonsense mutation in the enamelin gene causes local hypoplastic autosomal dominant amelogenesis imperfecta (AIH2). Hum. Mol. Genet. 11:1069–1074.
Massa, L. F., A. Ramachandran, A. George, and V. E. Arana-Chavez. 2005. Developmental appearance of dentin matrix protein 1 during the early dentinogenesis in rat molars as identified by high-resolution immunocytochemistry. Histochem. Cell Biol. 124:197–205.
Masuya, H., K. Shimizu, H. Sezutsu, Y. Sakuraba, J. Nagano, A. Shimizu, N. Fujimoto, A. Kawai, I. Miura, H. Kaneda, K. Kobayashi, J. Ishijima, T. Maeda, Y. Gondo, T. Noda, S. Wakana, and T. Shiroishi. 2005. Enamelin (*Enam*) is essential for amelogenesis: ENU-induced mouse mutants as models for different clinical subtypes of human amelogenesis imperfecta (AI). Hum. Mol. Genet. 14:575–583.
Matthee, C. A., J. D. Burzlaff, J. F. Taylor, and S. K. Davis. 2001. Mining the mammalian genome for artiodactyl systematics. Syst. Biol. 50:367–390.
McLeod, S. A., F. C. Whitmore, and L. G. Barnes. 1993. Evolutionary relationships and classification. Pages 45–70 *in* The bowhead whale (J. J. Burns, J. J. Montague, and C. J. Cowles, eds). The Society for Marine Mammalogy, Lawrence, Kansas.
Messenger, S. L., and J. A. McGuire. 1998. Morphology, molecules, and the phylogenetics of cetaceans. Syst. Biol. 47:90–124.
Miller, G. S. 1923. The telescoping of the cetacean skull. Smithsonian Misc. Coll. 76:1–71.
Mitchell, E. D. 1989. A new cetacean from the Late Eocene La Meseta Formation, Seymour Island, Antarctic Peninsula. Can. J. Fish. Aquat. Sci. 46:2219–2235.
Muizon, C. 1987. The affinities of *Notocetus vanbenedeni*, an Early Miocene platanistoid (Cetacea, Mammalia) from Patagonia, southern Argentina. Am. Mus. Nov. 2904:1–27.
Muizon, C. 1994. Are the squalodonts related to the platanistoids? Proc. San Diego Mus. Nat. Hist. 29:135–146.
Müller, K. 2005. SeqState: primer design and sequence statistics for phylogenetic DNA datasets. Appl. Bioinformatics 4:65–69.
Murphy, W. J., E. Eizirik, W. E. Johnson, Y. P. Zhang, O. A. Ryder, and S. J. O'Brien. 2001. Molecular phylogenetics and the origins of placental mammals. Nature 409:614–618.
Nikaido, M., H. Hamilton, H. Makino, T. Sasaki, K. Takahashi, M. Goto, N. Kanda, L. A. Pastene, and N. Okada. 2006. Baleen whale phylogeny and a past extensive radiation event revealed by SINE insertion analysis. Mol. Biol. Evol. 23:866–873.
Nishida, S., L. A. Pastene, M. Goto, and H. Koike. 2003. SRY gene structure and phylogeny in the cetacean species. Mammal Study 28:57–66.
Nishiwaki, M. 1972. General biology. Pages 3–204 *in* Mammals of the sea: Biology and medicine (S. Ridgway, ed.). Charles C. Thomas, Springfield, Illinois.
Nylander, J. A. A. 2004. MrModelTest v2. (Program distributed by the author, Uppsala, Sweden.)
Oelschläger, H. 1986. Comparative morphology and evolution of the otic region in toothed whales (Cetacea, Mammalia). Am. J. Anat. 177:353–368.
Omura, H. 1964. A systematic study of the hyoid bones in baleen whales. Sci. Rep. Whales Res. Inst. 18:149–170.
Orton, L. S., and P. F Brodie. 1987. Engulfing mechanics of fin whales. Can. J. Zool. 65:2898–2907.
Packard, E. L., and R. Kellogg. 1934. A new cetothere from the Miocene Astoria Formation of Newport, Oregon. Carnegie Inst. Washing. Publ. 447:1–62.
Pilleri, G., and O. Pilleri. 1989. *Balaenoptera siberi*, ein neuer balaenopterid (Cetacea) aus der Pisco-Formation Perus I. Pages 63–106 *in* Beitrage zur palaeontologie der cetaceen Perus I (G. Pilleri, ed.). Hirnanatomisches Institut der Universitat Bern Ostermundigen, Bern, Switzerland.
Pivorunas, A. 1977. The fibrocartilage skeleton and related structures of the ventral pouch of balaenopterid whales. J. Morph. 151:299–314.
Pivorunas, A. 1979. The feeding mechanisms of baleen whales. Am. Scient. 67:432–440.
Pritchard, G. B. 1939. On the discovery of a fossil whale in the older Tertiaries of Torquay, Victoria. Vic. Nat. 55:151–159.
Queralt, R., R. Adroer, R. Oliva, R. J. Winkfein, J. D. Retief, and G. H. Dixon. 1995. Evolution of protamine P1 genes in mammals. J. Mol. Evol. 40:601–607.
Raven, H. C. 1937. Notes on the taxonomy and osteology of two species of *Mesoplodon* (*M. europaeus* Gervais, *M. mirus* True). Am. Mus. Novit. 905:1–30.
Rice, D. W. 1989: Sperm whale, *Physeter macrocephalus* Linnaeus 1758. Pages 177–233 *in* Handbook of marine mammals, volume 4 (S. H. Ridgway and R. J. Harrison, eds.). London, Academic Press.
Ridewood, W. G. 1923. Observations on the skull in foetal specimens of whales of the genera *Megaptera* and *Balaenoptera*. Phil. Trans. R. Soc. Lond. B 211:209–272.
Ronquist, F., and Huelsenbeck, J. P. 2003. MrBayes 3: Bayesian phylogenetic inference under mixed models. Bioinformatics 19:1572–1574.
Roth, F. 1978. *Mesocetus argillarius* sp. n. (Cetacea, Mysticeti) from Upper Miocene of Denmark, with remarks on the lower jaw and the echolocation system in whale phylogeny. Zool. Scr. 7:63–79.
Rychel, A. L., T. W. Reeder, and A. Berta. 2004. Phylogeny of mysticete whales based on mitochondrial and nuclear data. Mol. Phylogenet. Evol. 32:892–901.
Sanders, A. E., and L. G. Barnes. 2002a. Paleontology of the Late Oligocene Ashley and Chandler Bridge Formations of South Carolina, 3: Eomysticetidae, a new family of primitive mysticetes (Mammalia: Cetacea). Smithsonian Contrib. Paleobiol. 93:313–356.
Sanders, A. E., and L. G. Barnes. 2002b. Paleontology of the Late Oligocene Ashley and Chandler Bridge Formations of South Carolina, 2: *Micromysticetus rothauseni*, a primitive cetotheriid mysticete (Mammalia: Cetacea). Smithsonian Contrib. Paleobiol. 93:271–293.
Sanderson, S. L., and R. Wassersug. 1993. Convergent and alternative designs for vertebrate suspension feeding. Pages 37–112 *in* The skull, volume 3 (J. Hanken and B. K. Hall, eds.). University of Chicago, Chicago.

Sasaki, T., M. Nikaido, H. Hamilton, M. Goto, H. Kato, N. Kanda, L. A. Pastene, Y. Cao, R. E. Fordyce, M. Hasegawa, and N. Okada. 2005. Mitochondrial phylogenetics and evolution of mysticete whales. Syst. Biol. 54:77–90.

Sasaki, T., M. Nikaido, S. Wada, T.K. Yamada, Y. Cao, M. Hasegawa, and N. Okada. 2006. *Balaenoptera omurai* is a newly discovered baleen whale that represents an ancient evolutionary lineage. Mol. Phylogenet. Evol. 41:40–52.

Sawamura, H., S. Otani, H. Ichishima, H. Ito, and H. Ishikawa. 2006. Features implying the beginning of baleen growth in aetiocetids. J. Vert. Paleo. 26(Suppl. to 3):120A.

Schulte, H. W. 1916. Anatomy of a fetus of *Balaenoptera borealis*. Mem. Am. Mus. Nat. Hist. 1:389–502.

Schulte, H. W. 1917. The skull of *Kogia breviceps* Blainv. Bull. Am. Mus. Nat. Hist. 37:361–404.

Simmons, M. P., and H. Ochoterena. 2000. Gaps as characters in sequence-based phylogenetic analyses. Syst. Biol. 49:369–381.

Slijper, E. J. 1962. Whales, 2nd edition. Cornell University Press, Ithaca, New York.

Sorenson, M. D. 1999. TreeRot, version 2c. Boston University, Boston, Massachusetts.

Steeman, M. E. 2007. Cladistic analysis and a revised classification of fossil and recent mysticetes. Zool. J. Linn. Soc. Lond. 150:875–894.

Struthers, J. 1889. On some points in the anatomy of a *Megaptera longimana*. J. Anat. Physiol. 23:308–335.

Swift, C. C., and L. G. Barnes. 1996. Stomach contents of *Basilosaurus cetoides*: Implications for the evolution of cetacean feeding behavior, and evidence for vertebrate fauna of epicontinental Eocene seas. 6th NAPC Abstracts, Paleo. Soc. Spec. Publ. 8:380.

Swofford, D. L. 2002. PAUP*: Phylogenetic analysis using parsimony. Version 4.0b. Sinauer Associates, Sunderland, Massachusetts.

Thewissen, J. G. M., and E. M. Williams. 2002. The early radiations of Cetacea (Mammalia): Evolutionary pattern and developmental correlations. Ann. Rev. Ecol. Syst. 33:73–90.

Thompson, J. D., D. G. Higgins, and T. J. Gibson. 1994. CLUSTAL W: improving the sensitivity of progressive multiple sequence alignment through sequence weighting, position-specific gap penalties and weight matrix choice. Nucleic Acids Res. 22:4673–4680.

Tomilin, A. G. 1967. Cetacea, vol. 9 Mammals of the USSR and adjacent countries (V.G. Heptner, ed.) Jerusalem: Israel Program for Scientific Translation (translated from Russian to English).

Uhen, M. 1998. Middle to Late Eocene basilosaurines and dorudontines. Pages 29–61 *in* The emergence of whales (J. G. M. Thewissen, ed.). Plenum, New York.

Uhen, M. 1999. New species of protocetid archaeocete whale, *Eocetus wardii* (Mammalia, Cetacea), from the Middle Eocene of North Carolina. J. Paleo. 73:512–528.

Uhen, M. 2004. Form, function, and anatomy of *Dorudon atrox* (Mammalia, Cetacea): An archaeocete from the Middle to Late Eocene of Egypt. Univ. Mich. Pap. Paleo. 34:1–222.

Uhen, M., and P. D. Gingerich. 2001. New genus of dorudontine archaeocete (Cetacea) from the Middle-to-Late Eocene of South Carolina. Mar. Mamm. Sci. 17:1–34.

Utrecht, W. L. V. 1965. On the growth of the baleen plate of the fin whale and the blue whale. Bijdr. Dierk. 35:3–38.

Walmsley, R. 1938. Some observations on the vascular system of a female fetal finback. Contrib. Embryol. 27:109–178.

Werth, A. J. 2000. Feeding in marine mammals. Pages 487–526 *in* Feeding (K. Schwenk, ed.). Academic, San Diego.

Werth, A. J. 2001. How do mysticetes remove prey trapped in baleen? Bull Mus. Comp. Zool. 156:189–203.

Werth, A. J. 2004. Models of hydrodynamic flow in the bowhead whale filter feeding apparatus. J. Exp. Biol. 207:3569–3580.

Williamson, G. R. 1973. Counting and measuring baleen and ventral grooves of whales. Sci. Rep. Whales Res. Inst. 25:279–292.

Winge, H. 1921. A review of the interrelationships of the Cetacea. Smithsonian Misc. Coll. 72:1–97.

Yablokov, A. V., V. M. Bel'kovitch, and V. I. Borisov. 1964. Whales and Dolphins. Izd-vo Nauka, Moscow. (Translated to English by Joint Publications Research Service for the U.S. Department of Commerce.)

Ye, L., Y. Mishina, D. Chen, H. Huang, S. L. Dallas, M. R. Dallas, P. Sivakumar, T. Kunieda, T. W. Tsutsui, A. Boskey, L. F. Bonewald, and J. Q. Feng. 2005. *Dmp1*-deficient mice display severe defects in cartilage formation responsible for a chondrodysplasia-like phenotype. J. Biol. Chem. 280:6197–6203.

Zhang, J. 2003. Evolution by gene duplication. Trends Ecol. Evol. 18:292–298.

First submitted 30 August 2006; reviews returned 9 November 2006; final acceptance 13 September 2007
Associate Editor: Ron DeBry
Editor-in-Chief: Rod Page

APPENDIX 1

Taxon Sampling for Dental Gene Matrix

Three of the genes that we sampled are SCPP genes that are necessary for the proper development of teeth in mammals (Kawasaki and Weiss, 2003). Published sequences of *DMP1*, *AMBN*, and *ENAM* for six mammalian species *(Bos taurus, Sus scrofa, Canis familiaris, Mus musculus, Rattus norvegicus, Homo sapiens)* were downloaded from Genbank and included in the dental gene matrix. The following DNA samples were used to PCR amplify and sequence segments of four SCPP gene exons from one perissodactyl, seven artiodactyl, four odontocete, and 12 mysticete taxa (also see matrix at MorphoBank [http://morphobank.geongrid.org]). Two individuals of *Balaenoptera acutorostrata* (minke whale) were sampled to represent North Atlantic and North Pacific populations. *Eubalaena glacialis* (Northeast Fisheries Science Center, Stranding Network; SWFSC Z13086) did not amplify for *ENAM* and was not included in our analyses. In sum, there were 31 OTUs in the dental gene matrix.

Perissodactyla
- *Tapirus indicus* (NYZS)

"Artiodactyla"
- *Choeropsis liberiensis* (NYZS)
- *Ovis dalli* (CRO)
- *Antilocapra americana* (CRO)
- *Tragulus napu* (NYZS)
- *Tayassu tajacu* (NYZS)
- *Camelus dromedarius* (NYZS)
- *Lama guanicoe* (NYZS)

Odontoceti
- *Physeter macrocephalus* (MIL)
- Ziphiidae (*Mesoplodon bidens* SWFSC Z3859; *Mesoplodon peruvianus* MIL)
- Delphinidae (*Lissodelphis borealis* SWFSC Z176; *Pseudorca crassidens* SWFSC Z38069)
- *Delphinapterus leucas* (SWFSC Z35275; NYZS)

Mysticeti
- *Megaptera novaeangliae* (SWFSC Z11727; MIL)
- *Balaenoptera acutorostrata* from North Pacific (SWFSC Z13091 from TMMC)
- *Balaenoptera acutorostrata* from North Atlantic (ARN)
- *Balaenoptera bonaerensis* (SWFSC Z23603 from SAM M15375)
- *Balaenoptera borealis* (SWFSC 30490; SWFSC 30493)
- *Balaenoptera edeni+brydei* (*Balaenoptera edeni+brydei* complex SWFSC Z11995)
- *Balaenoptera musculus* (SWFSC Z4502)
- *Balaenoptera physalus* (SWFSC Z26295)
- *Eschrichtius robustus* (SWFSC Z13090 from TMMC; SWFSC Z5750)
- *Caperea marginata* (SWFSC Z26572 from SAM ABTC27074; SWFSC Z5988)
- *Eubalaena japonica* (SWFSC Z13190)
- *Eubalaena australis* (SWFSC Z18928 from SAM M16470)
- *Balaena mysticetus* (SWFSC Z6985 from NSB)

Abbreviations for DNA sources: SWFSC (Southwest Fisheries Science Center, La Jolla, California, USA), SAM (South Australian Museum, Adelaide, Australia), TMMC (The Marine Mammal Center, Sausalito, California, USA), NSB (North Slope Borough, Barrow, Alaska, USA), NYZS (New York Zoological Society, New York, New York, USA),

MIL (M. Milinkovitch, Yale University; currently Free University of Brussels, Brussels, Belgium), ARN (Ú. Árnason, University of Lund), CRO (M. Cronin, Yale University, New Haven, Connecticut, USA).

Taxon Sampling for Supermatrix

Morphological data.—For the supermatrix analysis, the following specimens and published literature were used to code one "archaeocete," four (two extant, two extinct) odontocete, and 31 (11 extant, 20 extinct) mysticete taxa for 102 morphological characters (also see references in character descriptions [Appendix 2]). Additional morphological data for extant taxa were compiled from Arnold et al. (2005a). Note that *Balaenoptera edeni* and *Balaenoptera brydei* have been merged as a single OTU in our phylogenetic analyses. This follows Sasaki et al. (2006), who argued, based on analyses of mt genomes, that these species form a monophyletic group to the exclusion of other extant mysticetes. However, the taxonomy of these *Balaenoptera* species is not yet settled, so we executed phylogenetic analyses both with and without *B. edeni* + *B. brydei* included. Critical basal relationships were not perturbed by the removal of *B. edeni* + *B. brydei* from the supermatrix in parsimony searches.

"Archaeoceti"
- †*Zygorhiza kochii* USNM 11962

Odontoceti
- *Physeter macrocephalus* in Flower (1869)
- Ziphiidae (*Tasmacetus shepherdi* USNM 484878)
- †*Agorophius* (composite based on †*Agorophius pygmaeus* in Fordyce [1981] and †*Agorophius* sp. ChM PV4256, 5852)
- †*Squalodon calvertensis* in Kellogg (1923)

Mysticeti
- †*Janjucetus hunderi* in Fitzgerald (2006)
- †*Mammalodon colliveri* cast of NMV P199986 and in Fitzgerald (2006)
- †*Aetiocetus weltoni* UCMP 122900
- †*Aetiocetus cotylalveus* USNM 25210
- †*Aetiocetus polydentatus* AMP 12
- †*Chonecetus goedertorum* LACM 131146
- †*Eomysticetus whitmorei* ChM PV4253
- †*Diorocetus hiatus* USNM 16783, 23494
- †*Cetotherium rathkii* in Brandt (1873)
- †*Aglaocetus patulus* USNM 23690
- †*Cophocetus oregonensis* in Packard and Kellogg (1934)
- †*Isanacetus laticephalus* in Kimura and Ozawa (2002)
- †*Mixocetus elysius* LACM 882
- †*Parietobalaena palmeri* USNM 10668, 10677, 16119, 12697
- †*Pelocetus calvertensis* USNM 11976
- †"*Balaenoptera*" *gastaldii* MGPT 13802
- †"*Megaptera*" *hubachi* MB Ma 28570
- †"*Megaptera*" *miocaena* USNM 10300
- †*Parabalaenoptera baulinensis* CASG 66660
- †Eschrichtiidae new gen et sp. SDSNH 90517
- *Megaptera novaeangliae* MSNT 263, USNM 369982
- *Balaenoptera acutorostrata* LACM 54598, USNM 571236, MSNT 260
- *Balaenoptera bonaerensis* NSMT M-19792
- *Balaenoptera borealis* USNM 504244
- *Balaenoptera edeni* + *brydei* (*Balaenoptera edeni* + *brydei* complex NSMT M-33622)
- *Balaenoptera musculus* LACM 72562, MSNT 250
- *Balaenoptera physalus* MSNT 251, LACM 86020
- *Eschrichtius robustus* LACM 85980, 86047
- *Caperea marginata* USNM 550146, IRSNB 1536
- *Eubalaena* (*Eubalaena glacialis* LACM 51763, MSNT 303)
- *Balaena mysticetus* LACM 54475, 54479

Institutional abbreviations: AMP, Ashoro Museum of Paleontology, Ashoro-cho, Hokkaido, Japan; CASG, California Academy of Sciences, Department of Geology, San Francisco, California, USA; ChM, the Charleston Museum, Charleston, South Carolina, USA; IRSNB, Institute Royal de Sciences de Belgique, Brussels, Belgium; MB, Museum für Naturkunde, Humboldt–Universitat zu Berlin, Berlin, Germany; LACM, Natural History Museum of Los Angeles County, Los Angeles, California, USA; MGPT, Museo di Geologia e Paleontologia, Universita di Torino, Torino, Italy; MSNT, Museo di Storia Naturale e del Territoria de'll Universita di Pisa, Pisa, Italy; NMV, National Musuem of Victoria, Paleontology Collections, Victoria, Australia; NSMT, National Science Museum, Tokyo, Japan; SDSNH, San Diego Natural History Museum, San Diego, California, USA; UCMP, University of California Museum of Paleontology, Berkeley, California, USA; USNM, US National Museum, Washington, DC, USA.

Molecular data.—For the supermatrix, the following DNA samples were used to PCR amplify and sequence segments of 11 nuclear genes (*AMBN*, *ATP7A*, *BDNF*, *CSN2*, *DMP1*, *ENAM*, *PKDREJ*, *PRM1*, *KITLG*, *RAG1*, *STAT5A*) from two extant odontocete and 11 extant mysticete taxa; note that three of these loci are SCPP genes from the dental gene matrix (see above). Additional molecular data were compiled from the literature, including insertions of transposons (Nikaido et al., 2006), mt genomes (Árnason et al., 2004; Sasaki et al., 2005, 2006), satellite DNA sequences (Árnason et al., 1992), nuclear pseudogene sequences (Levenson and Dizon, 2003), autosomal intron/exon sequences (Rychel et al., 2004), and segments of three Y-linked genes (Nishida et al., 2003; Hatch et al., 2006). Taxa sampled for these genes are shown in Fig. 3 and in the supermatrix (Morphobank [http://morphobank.geongrid.org]).

Odontoceti
- *Physeter macrocephalus* (MIL)
- Ziphiidae (*Mesoplodon bidens* SWFSC Z3859; *Mesoplodon peruvianus* MIL; *Ziphius cavirostris* MIL)

Mysticeti
- *Megaptera novaeangliae* (SWFSC Z11727; MIL)
- *Balaenoptera acutorostrata* (SWFSC Z13091 from TMMC; ARN)
- *Balaenoptera bonaerensis* (SWFSC Z23603 from SAM M15375)
- *Balaenoptera borealis* (SWFSC 30490; SWFSC 30493)
- *Balaenoptera edeni+brydei* (*Balaenoptera edeni+brydei* complex SWFSC Z11995; SWFSC Z16039)
- *Balaenoptera musculus* (SWFSC Z4502)
- *Balaenoptera physalus* (SWFSC Z4767; SWFSC Z26295; ROS)
- *Eschrichtius robustus* (SWFSC Z13090 from TMMC; SWFSC Z5750)
- *Caperea marginata* (SWFSC Z26572 from SAM ABTC27074; SWFSC Z5988)
- *Eubalaena* (*Eubalaena japonica* SWFSC Z13190; *Eubalaena australis* SWFSC Z18928 from SAM M16470)
- *Balaena mysticetus* (SWFSC Z6985 from NSB)

Abbreviations for DNA sources: SWFSC (Southwest Fisheries Science Center, La Jolla, California, USA), SAM (South Australian Museum, Adelaide, Australia), TMMC (the Marine Mammal Center, Sausalito, California, USA), NSB (North Slope Borough, Barrow, Alaska, USA), MIL (M. Milinkovitch, Yale University; currently Free University of Brussels, Brussels, Belgium), ROS (H. Rosenbaum, New York Zoological Society, New York, New York, USA), ARN (Ú. Árnason, Lund University, Lund, Sweden).

APPENDIX 2

Morphological Character List

The following morphological characters were coded and utilized in the supermatrix analysis (characters that were ordered in some analyses are noted):

1. Rostral curvature in lateral aspect (Barnes and McLeod, 1984; Messenger and McGuire, 1998).
   0 = Straight; 1 = Slightly arched dorsoventrally; 2 = Moderately arched dorsoventrally; 3 = Strongly arched dorsoventrally (ordered).
2. Rostral transverse width at midpoint relative to condylobasal length (Uhen, 1999).
   0 = Very narrow (5–12%); 1 = Narrow (15–22%); 2 = Broad (24–31%); 3 = Very broad (>31%) (ordered).
3. Transverse slope of maxilla at midpoint (Deméré et al., 2005).
   0 = Flat (0° to 10° to 20°), 1 = Sloped (20-35°), 2 = Steep (>45°), 3 = Vertical (90°) (ordered).
4. Lateral margins of maxillae (modified from Barnes, 1990; McLeod et al., 1993).
   0 = Thick, 1 = Thin.

5. Premaxillary-maxillary suture (Geisler and Sanders, 2003).
   0 = Fused dorsally along the midline, 1 = Unfused.
6. Position of narial fossa (Deméré et al., 2005).
   0 = Well anterior to antorbital notch, 1 = Parallel with or just posterior to antorbital notch, 2 = Well posterior to antorbital notch (ordered).
7. Nasals, length relative to condylobasal length (Deméré et al., 2005).
   0 = Long (17-25%), 1 = Moderate (10-16%), 2 = Short (5-10%) (ordered).
8. Nasals, width relative to length (Deméré et al., 2005).
   0 = Slender (15-25%), 1 = Broad (26-45%), 2 = Very broad (46-70%), 3 = Extremely broad (>71%) (ordered).
9. Nasals, shape of anterior margin (Deméré et al., 2005).
   0 = U- or V-shaped (posteriorly directed), 1 = Straight, 2 = V-shaped (anteriorly directed).
10. Nasals, shape of posterior margin (Deméré et al., 2005).
    0 = Frontals extend into nasals (W-shaped), 1 = Frontals extend into nasals (finger-shaped), 2 = Frontals extend into nasals (U-shaped), 3 = Straight or nearly straight margin, 4 = Nasals extend into frontals (M-shaped), 5 = Nasals extend into frontals (U or V-shaped).
11. Nasals, dorsal surface (Deméré et al., 2005).
    0 = Flattened, 1 = Sagittal keel entire length, 2 = Sagittal keel anterior half.
12. Nasals, relative position of posteriormost edge (modified from Geisler and Sanders, 2003).
    0 = Anterior to supraorbital process of the frontal, 1 = Anterior border of supraorbital process of the frontal, 2 = Posterior half of supraorbital process of the frontal, 3 = Zygomatic process, 4 = Posterior temporal fossa (ordered).
13. Premaxilla, posterior process (Miller, 1923).
    0 = No contact with the frontals, 1 = Contacting frontals, 2 = Contacting frontals and forming robust ascending processes.
14. Posteriormost end of ascending process of premaxilla (modified from Geisler and Sanders, 2003).
    0 = Anterior to supraorbital process of the frontal, 1 = Anterior border of supraorbital process of the frontal, 2 = Posterior border of supraorbital process of the frontal, 3 = At level of anterior tip of zygomatic process, 4 = At level of posterior region of temporal fossa (ordered).
15. Posteriormost edge of ascending process of maxilla (modified from Geisler and Sanders, 2003).
    0 = Anterior to supraorbital process of frontal, 1 = Anterior border of supraorbital process of frontal, 2 = Posterior border of supraorbital process of frontal, 3 = At level of anterior tip of zygomatic process, 4 = At level of posterior region of temporal fossa (ordered).
16. Descending process of maxilla (modified from McLeod et al., 1993).
    0 = Present, 1 = Present as infraorbital plate, 2 = Absent.
17. Maxillary-frontal suture (Deméré et al., 2005).
    0 = Maxilla abuts frontal, 1 = Maxilla overrides anteromedial corner of supraorbital process, 2 = Maxilla overrides anterior portion of supraorbital process creating a pocket, 3 = Maxilla completely overrides frontal.
18. Ascending process of maxilla (Deméré et al., 2005).
    0 = Developed as bluntly-shaped triangular wedge, 1 = Developed as broad bar, exposed dorsally, 2 = Developed as narrow bar, exposed laterally, 3 = Absent, 4 = Broad maxilla, extending to lateral margin of frontal.
19. Lacrimal (Deméré et al., 2005).
    0 = Exposed laterally, 1 = Covered by frontal.
20. Ascending process of maxilla and anterior wing of parietal (Deméré et al., 2005).
    0 = Separate, 1 = Abutting or nearly-abutting, 2 = Short overlap, 3 = Long overlap, 4 = Overlying (ordered).
21. Frontal, postorbital process (McLeod et al., 1993; Uhen, 1998; Kimura and Ozawa, 2002).
    0 = Well-separated from zygomatic process, 1 = Abutting or nearly abutting zygomatic process.
22. Frontal, supraorbital process, size and shape (Miller, 1923).
    0 = Broad in anteroposterior dimension, short in transverse dimension, 1 = Moderately broad anteroposteriorly and moderately elongate transversely, 2 = Very narrow anteroposteriorly and very elongate transversely.
23. Frontal, supraorbital process, slope (Miller, 1923).
    0 = At level of vertex, 1 = Gradually sloping from vertex, 2 = Abruptly deflected below vertex (ordered).
24. Frontal, exposure on cranial vertex (Lindow, 2002).
    0 = Long exposure, 1 = Short exposure, 2 = Very short exposure (ordered).
25. Parietal, exposure on cranial vertex (Fordyce, 1984).
    0 = Long, 1 = Short, 2 = Parietal excluded from the vertex (ordered).
26. Parietal/frontal, interorbital region (Deméré et al., 2005).
    0 = Both large (parietal = frontal), 1 = Parietal > frontal, 2 = Frontal > parietal, 3 = Both reduced, 4 = Parietal excluded from interorbital region.
27. Apex of occipital shield (Deméré et al., 2005).
    0 = Extension posterior to temporal fossa, 1 = Extension to posterior half of temporal fossa, 2 = Extension to anterior half of temporal fossa, 3 = Extension to orbit, 4 = Extension anterior to orbit (ordered).
28. Occipital shield, shape of anterior margin (Deméré et al., 2005).
    0 = Rounded, 1 = Sharply triangular, 2 = Bluntly triangular, 3 = Broad with straight margins.
29. Occipital shield, lateral margins (Deméré et al., 2005).
    0 = Convex, 1 = Straight, 2 = Concave (ordered).
30. Squamosal, zygomatic processes (Deméré et al., 2005).
    0 = Parallel to sagittal plane, 1 = Divergent from sagittal plane.
31. Squamosal fossa (Deméré et al., 2005).
    0 = Large and well-developed, 1 = Reduced to absent.
32. Squamosal cleft (Deméré et al., 2005).
    0 = Absent, 1 = Present, contacts pterygoid, 2 = Present, contacts alisphenoid, 3 = Present, contacts parietal.
33. Squamosal, glenoid fossa and zygomatic process (McLeod et al., 1993; Messenger and McGuire, 1998).
    0 = Elevated, 1 = Depressed.
34. Squamosal, posterior width (exoccipital width relative to zygomatic width; Deméré et al., 2005).
    0 = 50-70%, 1 = 70-80%, 2 = >80% (ordered).
35. Foramen pseudo-ovale, construction (modified from Deméré et al., 2005).
    0 = Squamosal only, 1 = Squamosal and pterygoid, 2 = Pterygoid only.
36. Palate, shape (modified from McLeod et al., 1993; Messenger and McGuire, 1998).
    0 = Flat with no median keel, 1 = Median keel dividing palate into right and left concave surfaces.
37. Palate, maxillary window on infraorbital plate (Deméré et al., 2005).
    0 = Absent, 1 = Present.
38. Lateral nutrient foramina and sulci on palate (modified from Geisler and Sanders, 2003).
    0 = Absent, 1 = Present.
39. Palatines, posterior extension (Deméré et al., 2005).
    0 = Extend to internal nares, 1 = Extend to slightly overlap the pterygoids, 2 = Long overlap of pterygoids nearly reaching pterygoid fossa (ordered).
40. Palatines, anterior margin (Deméré et al., 2005).
    0 = Blunt or U-shaped, 1 = W-shaped.
41. Vomer, posterior position (Barnes, 1990; McLeod et al., 1993; Messenger and McGuire, 1998).
    0 = Not exposed on basicranium, 1 = Exposed on basicranium and covering basisphenoid-basioccipital suture.
42. Basioccipital crests (modified from Lindow, 2002).
    0 = Narrow transversely, 1 = Wide.
43. Paroccipital process, skull in ventral aspect (modified from Kimura and Ozawa, 2002).
    0 = Posterior to occipital condyles, 1 = Parallel with occipital condyles, 2 = Well anterior to occipital condyles (ordered).
44. Tympanic bulla, medial margin (McLeod et al., 1993).
    0 = Rounded/inflated dorsoventrally, 1 = Flattened dorsoventrally.

45. Tympanic bulla, median furrow (Geisler and Sanders, 2003).
0 = Absent, 1 = Notch on posterior edge, 2 = Continuous anteroposterior furrow.
46. Periotic, transverse elongation of pars cochlearis (Geisler and Luo, 1996).
0 = Absent, 1 = Present.
47. Periotic, lateral projection of anterior process (Geisler and Luo, 1996; Geisler and Sanders, 2003).
0 = Absent, 1 = Present and small, 2 = Present and robust, 3 = Present and hypertrophied.
48. Periotic, attachment for tensor tympani muscle (Geisler and Luo, 1996; Geisler and Sanders, 2003).
0 = Present as enlarged fossa, 1 = Present as groove, 2 = Absent or poorly developed.
49. Periotic, promontorial groove on medial side of pars cochlearis (promontorium) (Kimura and Ozawa, 2002).
0 = Absent, 1 = Present.
50. Periotic, suprameatal region (Luo and Gingerich, 1999).
0 = Broad concavity or fossa, 1 = Flat or nearly flat without concavity, 2 = Bulging and rugose.
51. Periotic, perilymphatic foramen (modified from Geisler and Luo, 1996; Geisler and Sanders, 2003).
0 = Confluent with fenestra rotunda, 1 = Narrowly separated from fenestra rotunda, 2 = Widely separated from fenestra rotunda (ordered).
52. Periotic, endocranial opening of facial nerve canal (Geisler and Luo, 1996; Kimura and Ozawa, 2002; Geisler and Sanders, 2003).
0 = With anterior fissure, 1 = Oval shaped, 2 = Circular.
53. Mandibular symphysis (Fitzgerald, 2006).
0 = Sutured, 1 = not sutured (ligamentous attachment in extant mysticetes).
54. Maxilla, geometry/arrangement of lateral nutrient foramina and associated sulci (this study).
0 = Posterior foramina with sulci radially arranged (no open maxillary groove) and anterior foramina with elongate sulci parasagittally arranged, 1 = Posterior foramina coincident with open maxillary groove with numerous short transverse sulci and anterior foramina with elongate sulci parasagittally arranged, 2 = Posterior foramina single, separate from open maxillary groove without well-developed sulci and anterior foramina with elongate sulci parasagittally arranged, 3 = Posterior foramina multiple (roughly in two rows) without well-developed sulci (no open maxillary groove) and anterior foramina with elongate sulci parasagittally arranged.
55. Mandible, neck (dorsal aspect; Deméré et al., 2005).
0 = Straight neck, 1 = Reflexed neck.
56. Mandible, ventromedial groove (Bisconti, 2000).
0 = Absent, 1 = Present.
57. Mandible, curvature of ramus, in dorsal aspect (McLeod et al., 1993; Messenger and McGuire, 1998).
0 = Laterally concave, 1 = Straight, 2 = Laterally convex (ordered).
58. Mandible, mandibular foramen size (modified from Barnes, 1990; McLeod et al., 1993).
0 = Large, 1 = Small.
59. Mandible, mandibular condyle orientation (modified from Kimura and Ozawa, 2002).
0 = Directed posteriorly, 1 = Directed dorsally, 2 = Directed posterolaterally.
60. Mandible, coronoid process (modified from Barnes and McLeod, 1984; McLeod et al., 1993).
0 = Large and spatulate, 1 = Finger-like and laterally deflected, 2 = Developed as coronoid crest, 3 = Developed as small knob and low crest, 4 = Developed as rounded process with low crest.
61. Mineralized teeth in adults (Geisler and Sanders, 2003).
0 = Present, 1 = Absent.
62. Teeth, heterodonty (this study).
0 = Anterior and post-canine teeth strongly heterodont; 1 = Anterior and post-canine teeth moderately heterodont; 2 = Anterior and post-canine teeth weakly heterodont, 3 = Homodont dentition (ordered).
63. Vertebrae, cervical (Deméré et al., 2005).
0 = Unfused, 1 = Up to 6 vertebrae fused, 2 = All 7 vertebrae fused as compact unit (ordered).
64. Scapula, acromion process (modified from Muizon, 1994).
0 = Large, 1 = Reduced or absent.
65. Scapula, coracoid process (Miller, 1923; Muizon, 1987).
0 = Present, 1 = Absent.
66. Humerus-radius length ratio (modified from Kimura and Ozawa, 2002).
0 = Humerus equal or longer than radius, 1 = Humerus shorter than radius.
67. Manus, number of digits (Barnes and McLeod, 1984; Messenger and McGuire, 1998).
0 = 5 digits, 1 = 4 digits.
68. Dorsal fin (Geisler and Sanders, 2003).
0 = Present, 1 = Dorsal humps, 2 = Absent.
69. Ventral grooves (modified from Tomilin, 1967).
0 = Absent, 1 = 2-10, confined to throat region, 2 = Numerous and terminate midbody, 3 = Numerous and extend at or posterior to the umbilicus.
70. Ventral throat pouch (Schulte, 1916).
0 = Absent, 1 = Present.
71. Baleen (Geisler and Sanders, 2003).
0 = Absent, 1 = Present.
72. Baleen, thickness (Werth, 2001).
0 = Thin and flexible, 1 = Thick and rigid.
73. Baleen, length and width (Messenger and McGuire, 1998; Werth, 2001).
0 = Baleen extremely long (>15% of body length) and laterally compressed, 1 = Baleen significantly shorter (<6% of body length) and wider.
74. Baleen, fringe (Werth, 2000, 2001).
0 = Fine, 1 = Coarse.
75. Tongue (Sanderson and Wassersug, 1993).
0 = Muscular, 1 = Reduced and predominantly connective tissue.
76. Longitudinal ridges on rostrum (Omura, 1964).
0 = Absent or indistinct, 1 = Single, median ridge, 2 = Three longitudinal ridges (ordered).
77. Teeth, number of upper molars (Uhen and Gingerich, 2001).
0 = Two, 1 = Three, 2 = More than three (ordered).
78. Maxilla, antorbital notch (Fordyce, 1981; Heyning, 1989).
0 = Open, 1 = Closed (V-shaped invagination).
79. Frontal, temporal crest (attachment for temporalis muscle) (Geisler and Sanders, 2003).
0 = Does not extend far onto dorsal surface of supraorbital process of frontal, 1 = Does extend far onto dorsal surface of supraorbital process of frontal.
80. Pterygoid (Fraser and Purves, 1960).
0 = Small with poorly developed hamular process, 1 = Small with robust hamular process, 2 = Large with small hamular process.
81. Mandible, position of coronoid process (Bisconti and Varola, 2000).
0 = Located relatively close to mandibular condyle, 1 = Located relatively far anterior to mandibular condyle.
82. Mandible, postcoronoid elevation (Kimura, 2002).
0 = Absent, 1 = Present.
83. Mandible, shape of mandibular condyle (Winge, 1921).
0 = Transversely expanded and slightly cylindrical, 1 = Bulbous and spherical, 2 = Transversely compressed and ovoid.
84. Mandible, orientation of the angle (Bisconti and Varola, 2000; Kimura, 2002).
0 = Posteriorly, 1 = Posteroventrally.
85. Mandible, proportional size of mandibular angle relative to mandibular condyle in the dorsoventral plane (modified from Bisconti and Varola, 2000; Kimura, 2002).
0 = Angle larger than condyle, 1 = Angle and condyle similar in size, 2 = Angle half the size of condyle, 3 = Angle severely reduced (ordered).
86. Mandible, subcondylar furrow (Roth, 1978).
0 = Absent, 1 = Present.
87. Mandible, relative position of anterior border of mandibular foramen (Struthers, 1889; Roth, 1978).
0 = Anterior to coronoid process, 1 = In line with middle of coronoid process, 2 = In line with posterior edge of coronoid process, 3 = Posterior to coronoid process (ordered).

88. Mandible, ventral surface of middle portion of mandible (Deméré, 1986; Kimura and Ozawa, 2002).
    0 = Rounded, 1 = Blade-like keel.
89. Mandible, medial torsion of the anterior portion (Deméré, 1986; Sanders and Barnes, 2002a).
    0 = Absent, 1 = Present.
90. Sternum (Yablokov et al., 1964; Nishiwaki, 1972).
    0 = Sternum large, composed of several bones and articulating with more than one rib, 1 = Sternum small, composed of one bone, and articulating with one rib.
91. Hyoid, curvature of fused basihyal-thyrohyal (Omura, 1964).
    0 = Strongly curved, straight length less than 75% of curved length, 1 = Straight length between 75–90% of curved length (slightly curved), 2 = Straight length more than 90% of curved length (ordered).
92. Hyoid, ankylosed basihyal and thyrohyals (Omura, 1964).
    0 = Absent or absent in younger individuals, 1 = Present at all stages.
93. Hyoid, anterior processes (Omura, 1964).
    0 = Absent, 1 = Short and robust, 2 = Long and slender.
94. Hyoid, fossa between anterior processes (this study).
    0 = Absent, 1 = Present.
95. Parietal-frontal suture, anterior extension (this study).
    0 = None, 1 = Lobate and separated from median rostral elements, 2 = Triangular and separated from median rostral elements, 3 = Lobate and overlapping median rostral elements.
96. Palatal window exposing vomer (this study).
    0 = Absent, 1 = Present.
97. Palatine notch (this study).
    0 = Absent, 1 = Present.
98. Posterior sinus (modified from Oelschläger, 1986).
    0 = Poorly developed or absent, 1 = Present.
99. Posterior teeth, root condition (this study).
    0 = Two rooted with fused roots, 1 = Double rooted, 2 = Single rooted.
100. Procumbent anterior teeth relative to posterior teeth (this study).
    0 = Absent, 1 = Present.
101. Enamel on postcanine teeth with vertical striations (this study).
    0 = On lingual surface only, 1 = Very heavy on lingual and labial surfaces, 2 = Poorly developed or absent.
102. Anterior and posterior denticles on posterior upper teeth (this study).
    0 = 5 or more, large and well developed, 1 = 3 or fewer, small and simple, 2 = Denticles absent (ordered).